AD_____

Award Number: DAMD17-03-1-0024

TITLE: Activation of Polyamine Catabolism as a Novel Strategy for Treating and/or Preventing Human Prostate Cancer

PRINCIPAL INVESTIGATOR: Carl W. Porter, Ph.D.

CONTRACTING ORGANIZATION: Health Research, Incorporated
Roswell Park Cancer Institute Division
Buffalo, New York 14263

REPORT DATE: March 2005

TYPE OF REPORT: Annual

PREPARED FOR: U.S. Army Medical Research and Materiel Command
Fort Detrick, Maryland 21702-5012

REPORT DOCUMENTATION PAGE

Form Approved
OMB No. 074-0188

1. AGENCY USE ONLY (Leave blank)	2. REPORT DATE	3. REPORT TYPE AND DATES COVERED
	March 2005	Annual (1 Mar 04 - 28 Feb 05)

4. TITLE AND SUBTITLE
Activation of Polyamine Catabolism as a Novel Strategy for Treating and/or Preventing Human Prostate Cancer

5. FUNDING NUMBERS
DAMD17-03-1-0024

6. AUTHOR(S)
Carl W. Porter, Ph.D.

7. PERFORMING ORGANIZATION NAME(S) AND ADDRESS(ES)
Health Research, Incorporated
Roswell Park Cancer Institute Division
Buffalo, New York 14263

E-Mail: carl.porter@roswellpark.org

8. PERFORMING ORGANIZATION REPORT NUMBER

9. SPONSORING / MONITORING AGENCY NAME(S) AND ADDRESS(ES)
U.S. Army Medical Research and Materiel Command
Fort Detrick, Maryland 21702-5012

10. SPONSORING / MONITORING AGENCY REPORT NUMBER

11. SUPPLEMENTARY NOTES
Original contains color plates: All DTIC reproductions will be in black and white.

12a. DISTRIBUTION / AVAILABILITY STATEMENT
Approved for Public Release; Distribution Unlimited

12b. DISTRIBUTION CODE

13. ABSTRACT (Maximum 200 Words)

The relationship of polyamines to the prostate is unique among all tissues since, in addition to synthesizing these molecules for cell growth, the gland produces massive quantities for export into semen. It might, therefore, be expected that prostatic tumors could exhibit atypical polyamine-related regulatory responses. We propose that activation of polyamine catabolism may have unique therapeutic potential against prostate carcinoma. Thus far, we have validated this hypothesis by demonstrating that (a) conditional overexpression of the polyamine catabolic enzyme spermidine/spermine N^1-acetyltransferase (SSAT) causes growth inhibition in LNCaP prostate carcinoma cells and (b) cross-breeding of SSAT transgenic mice with prostate cancer prone TRAMP mice markedly suppresses genitourinary tumor development via an apparent depletion of the SSAT cofactor acetyl-CoA. Depletion of the critical metabolite, acetyl-CoA, appears to be responsible for a selective effect on the prostate and prostate proliferative disease. The ultimate goal of these studies is to genetically validate the concept that small molecule induction of SSAT represents a promising anticancer strategy against prostate cancer and that it is worthy of small molecule discovery and development.

14. SUBJECT TERMS
acetyl-CoA, LNCaP cells, polyamines, prostate, SSAT, TRAMP mice

15. NUMBER OF PAGES
36

16. PRICE CODE

17. SECURITY CLASSIFICATION OF REPORT	18. SECURITY CLASSIFICATION OF THIS PAGE	19. SECURITY CLASSIFICATION OF ABSTRACT	20. LIMITATION OF ABSTRACT
Unclassified	Unclassified	Unclassified	Unlimited

TABLE OF CONTENTS

DAMD17-03-1-0024

REPORT BODY ***(Tables & Figures located in Appendix 1)***

***A. Introduction*:**

Polyamines are organic cations found in all cells and known to be essential for the initiation and maintenance of cell growth. As such, polyamine biosynthesis has been targeted as an anticancer strategy. The relationship of polyamines to the prostate is unique among all tissues since in addition to synthesizing these molecules for cell growth, the gland produces massive quantities for export into semen. It might, therefore, be expected that prostatic tumors could exhibit atypical polyamine-related regulatory responses (1). In recognition of the unique physiology of the prostate gland, Heston and collaborators proposed that targeting polyamine biosynthesis may be particularly effective against prostate cancer (2). Although most of these efforts have focused on inhibition of polyamine biosynthesis, we propose that activation of polyamine catabolism may have unique therapeutic potential against prostate carcinoma. The concept derives from our studies with polyamine analogs where, for example, we have shown that polyamine analogs such as N^1,N^{11}-diethylnorspermine (DENSPM) down-regulate polyamine biosynthesis at the level of ornithine decarboxylase (ODC) and S-adenosylmethionine decarboxylase (SAMDC) and at the same time, potently (i.e. >200-fold) up-regulate polyamine catabolism at the level of spermidine/spermine N^1-acetyltransferase (SSAT, 3). Several lines of evidence support the idea that analog induction of SSAT and hence, activation of polyamine catabolism, is a critical determinant of DENSPM drug action. (4-10). These various studies relate to SSAT induction in the context of analog treatment but they do not address what happens when SSAT is selectively induced in cells. In the absence of a specific SSAT inducer, this could only be evaluated using genetic systems such as conditional overexpression as a means to mimic small molecule induction of the enzyme. We have previously shown that conditional overexpression of SSAT leads to polyamine pool depletion and growth inhibition in MCF-7 breast carcinoma cells. On the basis of rationale suggesting that prostate carcinoma may be more sensitive to perturbations in polyamine homeostasis, we proposed to investigated the metabolic and antiproliferative consequences of conditional SSAT overexpression in *in vitro* and transgenic overexpression in *in vivo* systems. *The bottom-line goal of these studies is to genetically validate the concept that small molecule induction of SSAT is a useful anticancer strategy against prostate cancer and thus, worthy of small molecule discovery and development.* On the basis of findings to date, activation of polyamine catabolism, as opposed to inhibition of polyamine biosynthesis, represents a viable polyamine-directed anticancer strategy for prostate cancer.

B. *Progress according to task:*

Task 1. *To evaluate the cellular and metabolic consequences of conditional SSAT over-expression in cultured LNCaP cells as a means to genetically validate the antiproliferative potential of this strategy .*

The bulk of this Task was carried out in Year 1. In year two, we completed the necessary work and refinement of previous work to publish this in Journal of Biological Chemistry (12, see Appendix). On the basis of findings with polyamine analogs, we hypothesized that activation of the polyamine catabolism at the level of SSAT will also inhibit cell growth. To summarize this work, SSAT was conditionally over-expressed in LNCaP prostate carcinoma cells via a

tetracycline-regulatable (Tet-off) system. Tetracycline removal resulted in a rapid ~10-fold increase in SSAT mRNA and a ~20-fold increase in enzyme activity. Consistent with this response, high levels of the SSAT products N^1-acetylspermidine, N^1-acetylspermine and N^1,N^{12}-diacetylspermine were found to accumulate both intracellularly and extracellularly. SSAT induction led to significant growth inhibition which in contrast to MCF-7 cells (11), was not accompanied by polyamine pool depletion. Rather, intracellular spermidine and spermine pools were elevated or maintained at control levels by a robust compensatory increase in biosynthesis at the levels of ODC and SAMDC activities. This, in turn, gave rise to a high rate of metabolic flux through both the biosynthetic and catabolic pathways—a new concept in polyamine biology (Figure 1). Interruption of that flux with α-difluoromethylornithine (DFMO), an inhibitor of ODC and well-known antiproliferative agent, unexpectedly prevented growth inhibition during Tet removal. As diagramed in our newly revised figure for metabolic flux (see Figure 1), it appears that flux-induced growth inhibition may derive from excess product accumulation (i.e. acetylated polyamines) and/or to metabolite depletion such as a ~50% reduction in *S*-adenosylmethionine (SAM) pools or a ~50% decrease in the SSAT cofactor acetyl-CoA. In summary, the results demonstrate that activation of polyamine catabolism by conditional SSAT overexpression leads to: (a) altered polyamine pool homeostasis (b) a compensatory increase in polyamine biosynthesis, (c) heightened metabolic flux through both the biosynthetic and catabolic pathways, (d) depletion of metabolite pools such as the polyamine precursor SAM and the SSAT cofactor, acetyl-coenzyme A (acetyl-CoA) and (e) rapid and sustained growth inhibition. Whether these responses are unique to prostate derived tumor cells remains to be demonstrated. Overall, this important study shows that activation of polyamine catabolism gives rise to growth inhibition and thereby provides genetic validation of the idea that small molecule induction of SSAT may be effective as an anticancer strategy for treating prostate cancer.

We are continuing to utilize the LNCaP model system developed in this Task to attempt to determine which of the variables affected by polyamine flux (Figure 1) is directly responsible for inhibition of cell growth. The design of these studies involves activating SSAT and examining variables affected by concomitant DFMO treatment which rescues growth inhibition. The intention is to identify those variables which are affected by SSAT alone and are rescued with DFMO treatment. This is modeled after a previously submitted Figure which can be now seen as Figure 7 in Kee *et al.* (12; see Appendix).

Task 2. *To determine the generality of cellular and metabolic consequences seen in Task 1 on representative prostate cancer cell lines in which SSAT has been adenovirally transduced.*

We have previously successfully prepared and purified a SSAT expressing adenovirus in which human SSAT cDNA and GFP. The goal of these studies was to use the adenovirus to transduce SSAT into a number of prostate cancer cell lines and examine the effects on polyamine metabolism and cell growth. An unexpected complication was that while the SSAT adenovirus could be used to transduce SSAT into 293 cells in the absence of toxicity, this was not the case with LNCaP or PC-3 cells which were cytotoxically affected. In view of these unforeseen difficulties and in consideration of the success of Task 3, we submitted in 2004 a shift in work (SOW) request in which we proposed to abandon Task 2 and focus on additional cross-breeding opportunities under Task 3. These include making use of genetically altered mice currently that are now under development in the Porter laboratory. The SOW to do this work was approved and we are expanding our efforts in Task 3 to include genetic crosses with these new mice as they become available. In the past cycle, we began crossing TRAMP mice with SSAT knock-out mice and ODC heterozygous mice (see Task 3).

Task 3. *To confirm that responses to SSAT over-expression seen in vitro (as determined in Tasks 1 and 2) are translatable to antitumor activity in vivo.*

As noted in Task 1, we have previously reported that activation of polyamine catabolism via conditional overexpression of SSAT has antiproliferative consequences in LNCaP prostate carcinoma cells growing in culture (12). In this Task, we sought to examine the *in vivo* consequences of SSAT overexpression in a mouse model for prostate cancer. Although much of these studies were completed in year 1, we spent the past year accumulating the necessary data for publication in the Journal of Biological Chemistry (13, see Appendix). This included quantitation of prostate and liver SSAT gene expression in mouse cohorts of the SSAT / TRAMP cross (Figure 2), confirming that the tumor suppressive effect of SSAT extended beyond 30 wks (Figure 3C), investigating the effects of SSAT-induced metabolic flux on acetyl-CoA and S-adenosylmethionine pools (Figure 4), and documenting the loss of abdominal and subdermal fat in SSAT transgenic mice as support for the effects of metabolic flux on acetyl-CoA pools (Figure 5). The following summary of this two year effort takes this newly acquired data into account. TRAMP (TRansgenic Adenocarcinoma of the Mouse Prostate) female C57BL/6 mice that express the SV40 early genes (T/t antigens) under an androgen-driven probasin promoter (14) were cross-bred with male C57BL/6 transgenic mice that systemically over-express SSAT (15). Experiments were staged by small animal nuclear magnetic resonance image (MRI) tracking of tumor appearance and growth. At 30 weeks of age (Figure 3), the average genitourinary tract weights for TRAMP mice were 1,417 ± 181 mg compared to 344 ± 52 mg for TRAMP/SSAT mice (Figure 3). Thus, transgenic overexpression of SSAT suppressed outgrowth of prostate tumors. Since this could represent a delay in tumor development, we examined the effects at a later age. By 36 wk, the average TRAMP genitourinary tract increased by ~2-fold relative to the 30 wk data while those of TRAMP/SSAT actually decreased by 33% as opposed to growing larger (Figure 3). Since the differential effect increased between groups, we conclude that the tumor suppressive effect was not temporary but rather progressive. Immunohistochemistry revealed that SV40 large T-antigen expression in the prostate epithelium was similar in TRAMP versus TRAMP/SSAT mice indicating that the driving oncogene was intact and unaffected. Consistent with the 18-fold increase in SSAT activity in the TRAMP/SSAT transgenics, intracellular N^1-acetylspermidine and putrescine pools were markedly increased (i.e. 35-fold and 16-fold, respectively) relative to the TRAMP mice while spermidine and spermine pools were largely unaffected due to a compensatory 5- to 7-fold increase in the biosynthetic enzyme activities of ODC and SAMDC. The latter led to heightened metabolic flux through the polyamine pathway and an associated ~70% reduction in the SSAT cofactor acetyl-CoA and a ~40% reduction in the polyamine aminopropyl donor S-adenosylmethionine in TRAMP/SSAT compared to TRAMP prostatic tissue. In addition to elucidating the antiproliferative and metabolic consequences of SSAT overexpression in a prostate cancer model, these findings provide genetic support for the discovery and development of specific small molecule inducers of SSAT as a novel therapeutic strategy targeting prostate cancer. On the basis of these findings, Dr. Porter was recently awarded a NCI RAND grant to search by high throughput screening of the NCI compound library for specific small molecule inducers of SSAT as an anticancer agent leads. Given the fact that transgenic overexpression of SSAT affected normal prostates of mice as well as neoplastic prostates, such compounds may find usefulness in treating prostatic hyperplasia.

In addition to the antitumor implications, the findings of Task 1 and 3 provide the first definitive linkage between polyamine catabolism and fat metabolism via the SSAT coenzyme acetyl-CoA. The finding is strongly supported by the observations that SSAT-transgenic mice

lack fat (Figure 5) and a significant proportion (i.e. ~33%) of SSAT-knock-out mice accumulate fat (data not shown). The latter finding has important implications for a possible role of SSAT in fat homeostasis, a lead that will be explored under other funding mechanisms. At a minimum, it is consistent with recent strategies by other groups to use interference with fat biosynthesis (i.e. fatty acid synthase inhibitors) as an anticancer approach to prostate cancer (16).

To compliment the above findings, we initiated studies in which SSAT null mice were crossed with TRAMP mice (16) and observed that null expression of the enzyme had no effect on prostate tumor growth (Figure 6). Preliminary biochemical analysis of various tissues including prostate and prostate tumors mice failed to show any major perturbations of polyamine metabolism (data not shown). Taken together, the findings are consistent with the SSAT transgenic studies and further, imply that there is no therapeutic merit for SSAT-inhibition as an anticancer strategy in prostate. While waiting for additional genetically altered mice to be developed (see below), we have also examined the effects of ODC heterozygosity on tumorigenesis in the TRAMP mouse since a decrease in biosynthesis might mimic an increase in catabolism via SSAT. These are relatively difficult crosses but on the basis of animals obtained thus far, it appears that ODC haploinsufficiency actually enhances prostate tumorigenesis in the TRAMP mouse (Figure 7). Further, the tumors tend to be more restricted to the prostate gland and they do not move out into the seminal vesicles as is typical of tumors in the C57 Bl/6 TRAMP background. Preliminary biochemical findings on various tissues including prostate tumors from TRAMP and TRAMP/ODC$^{+/-}$ show no major perturbations in polyamine metabolism despite a reduction in ODC gene dose (data not shown). The promoting effect of ODC heterozygosity on tumorigenesis is highly unexpected based on the known role of this enzyme in carcinogenesis and tumor growth and the finding may reflect something unique about the context of prostate cells and tissue.

Based on our success with SSAT and consistent with our earlier SOW for Task 2, we plan to cross-breed TRAMP mice with mice that transgenically over express other polyamine catabolic enzymes (17-19). Our laboratory was first to report on the genomic identification and biochemical characterization of two such enzymes, PAO and a previously unknown enzyme, spermine oxidase SMO (18). We are now attempting to derive mice that transgenically over express these polyamine catabolic enzymes. These will then be used to extend studies in Task 3 as described in the SOW for Task 2. Thus far, we have derived founder transgenic animals for both enzymes but unfortunately, the transgenic SMO mice did not over-express the enzyme at the level of protein or mRNA. Offspring of the transgenic PAO founder mice were recently analyzed and found to over express the enzyme protein only in the muscle and kidney and thus it is not useful for our prostate studies.

We have also undertaken to determine whether the antitumor effect of activated polyamine catabolism as seen in the TRAMP mouse model can be applied to other tumor types. Stated otherwise, we sought to determine if the tumor suppression seen in the TRAMP mouse was unique to prostate cancer. Thus, we have begun a collaboration with Dr. Frank Berger (University of South Carolina) studying the *APC^{min}* mice which are genetically predisposed to develop intestinal tumors. Since the bulk of this work was done by Dr. Berger, we did not feel that a SOW was necessary. Initial findings indicate that when crossed with SSAT transgenics, these mice develop a significantly increased (rather than decreased) number of intestinal polyps (Figure 8). Further documentation including crossing the *APC^{min}* mice with SSAT knock out mice is underway. The difference relative to the findings in the prostate suggests that tissue and metabolic contexts may

play a major role in determining the nature of the tumor response to activated polyamine catabolism. It also raises considerations relating to the therapeutic potential of this approach. At a minimum, however, these findings strongly implicate differential roles for SSAT in tumorigenesis.

C. Key Research Accomplishments:

- Publication of a report showing that cross-breeding SSAT transgenic mice with TRAMP mice that are genetically predisposed to prostate cancer, markedly suppresses tumor development. The extent of the effect is greater than seen with any previously reported cross-breeding of TRAMP mice (see Kee *et al.*, 12)
- We are now able to detect and quantitate acetyl-CoA as well as malonyl-CoA (a major regulator of fat oxidation) by capillary electrophoresis, which will be used to study the downstream consequences of SSAT-induced metabolic flux (unpublished) and how it relates to growth inhibition in the LNCaP cell system.
- Publication of a report showing that the suppression of tumorigenesis in TRAMP mice crossed with SSAT transgenics, appears to be due to increased metabolic flux through the polyamine pathway due to SSAT over-expression. The increased flux in turn correlates with reductions in the SSAT cofactor, acetyl-CoA and this aligns with phenotypic features (lack of fat) of the SSAT mouse. This supports the earlier in vitro findings of this grant and together they represent the first linkage between polyamine metabolism and fat homeostasis (see Kee *et al.*, 13).
- Cross-breeding of TRAMP mice with SSAT null mice appears to have minimal effect on prostate tumorigenesis while cross-breeding to achieve ODC heterozygosity appears to promote TRAMP tumorigenesis.
- In collaborative studies, we found that cross-breeding of SSAT transgenic mice with APC^{min} mice promotes intestinal tumorigenesis which is opposite to the effect seen in the TRAMP model. The findings demonstrate the apparent importance of genetic context in the SSAT response although it is not yet clear what specific factor constitutes the basis for this difference. The findings also reinforce the importance of the SSAT gene in tumor biology.

D. Reportable Outcomes: **Reprints attached in Appendix**

-
- Kee, K., Vujcic, S., Merali, S., Diegelman, P., Kisiel, N., Powell, C.T., Kramer, D.L. and Porter, C.W. Metabolic and antiproliferative consequences of activated polyamine catabolism in LNCaP prostate carcinoma cells. J. Biol. Chem. 279:27050-27058, 2004.
- Kee, K., Foster, B.A., Merali, S., Vujcic, S.,, Mazurchuk, R., Hensen, M.L., Diegelman, P., Kisiel, N., Kramer, D.L., and Porter, C.W. Activated polyamine catabolism depletes acetyl-CoA and suppresses prostate tumor growth in the TRAMP mouse. J. Biol. Chem. 279:40076-40083, 2004

E. Conclusions:

We have genetically validated that activated polyamine catabolism at the level of SSAT has profound antitumor effects against prostate cancer at both the *in vitro* and *in vivo* levels. These finding provide genetic evidence for the concept that selective small molecule induction of SSAT may be effective in treating prostate hyperplasia and cancer. The findings further defines the downstream metabolic consequences of this strategy include marked reduction of acetyl-CoA pools in a manner that correlates very closely with suppression of tumor growth. This is the first recognition of a biological consequence deriving from altered flux through the polyamine pathway. Since this seems to occur selectively in both the normal and neoplastic prostate and since the phenotypic consequences of sustained transgenic overexpression of SSAT include only hair loss and female infertility, a small molecule induction of SSAT would appear to be selectively directed at prostate disease. Lastly, we have clearly shown that the *in vivo* antitumor responses to perturbations in SSAT activity are highly dependent on tissue and metabolic context with prostate tumors being sensitive to induction of SSAT.

F. References:

1. Mi, Z., Kramer, D. L., Miller, J. T., Bergeron, R. J., Bernacki, R., and Porter, C. W. Human prostatic carcinoma cell lines display altered regulation of polyamine transport in response to polyamine analogs and inhibitors. Prostate, *34:* 51-60, 1998.
2. Heston, W. D. Prostatic polyamines and polyamine targeting as a new approach to therapy of prostatic cancer. Cancer Surveys, *11:* 217-238, 1991.
3. Porter, C. W., Regenass, U., and Bergeron, R. J. Polyamine inhibitors and analogs as potential anticancer agents. *In:* R. H. Dowling, U. R. Folsch, and C. Loser (eds.), Falk Symposium on Polyamines in the Gastrointestinal Tract, pp. 301-322. Dordrecht, Netherlands: Kluwer Academic Publishers Group, 1992.
4. Casero, R. A., Jr., Celano, P., Ervin, S. J., Porter, C. W., Bergeron, R. J., and Libby, P. R. Differential induction of spermidine/spermine N^1-acetyltransferase in human lung cancer cells by the bis(ethyl)polyamine analogues. Cancer Res, *49:* 3829-3833, 1989.
5. Shappell, N. W., Miller, J. T., Bergeron, R. J., and Porter, C. W. Differential effects of the spermine analog, N^1,N^{12}-bis(ethyl)-spermine, on polyamine metabolism and cell growth in human melanoma cell lines and melanocytes. Anticancer Res, *12:* 1083-1089, 1992.
6. Pegg, A. E., Wechter, R., Pakala, R., and Bergeron, R. J. Effect of N^1,N^{12}-bis(ethyl)spermine and related compounds on growth and polyamine acetylation, content, and excretion in human colon tumor cells. J Biol Chem, *264:* 11744-11749, 1989.
7. Porter, C. W., Ganis, B., Libby, P. R., and Bergeron, R. J. Correlations between polyamine analogue-induced increases in spermidine/spermine N^1-acetyltransferase activity, polyamine pool depletion, and growth inhibition in human melanoma cell lines. Cancer Res, *51:* 3715-3720, 1991.
8. McCloskey, D. E. and Pegg, A. E. Altered spermidine/spermine N^1-acetyltransferase activity as a mechanism of cellular resistance to bis(ethyl)polyamine analogues. J Biol Chem, *275:* 28708-28714, 2000.
9. Chen, Y., Kramer, D. L., Li, F., and Porter, C. W. Loss of inhibitor of apoptosis proteins as a determinant of polyamine analog-induced apoptosis in human melanoma cells. Oncogene, *22:* 4964-4972, 2003.

10. Chen, Y., Kramer, D. L., Jell, J., Vujcic, S., and Porter, C. W. Small interfering RNA suppression of polyamine analog-induced spermidine/spermine N^1-acetyltransferase. Mol Pharmacol, *64:* 1153-1159, 2003.
11. Vujcic, S., Halmekyto, M., Diegelman, P., Gan, G., Kramer, D. L., Janne, J., and Porter, C. W. Effects of conditional overexpression of spermidine/spermine N^1-acetyltransferase on polyamine pool dynamics, cell growth, and sensitivity to polyamine analogs. J Biol Chem, *275:* 38319-38328, 2000.
12. Kee, K., Vujcic, S., Merali, S., Diegelman, P., Kisiel, N., Powell, C.T., Kramer, D.L. and Porter, C.W. Metabolic and antiproliferative consequences of activated polyamine catabolism in LNCaP prostate carcinoma cells. J. Biol. Chem. 279:27050-27058, 2004. (see Appendix)
13. Kee, K., Foster, B.A., Merali, S., Vujcic, S.,, Mazurchuk, R., Hensen, M.L., Diegelman, P., Kisiel, N., Kramer, D.L., and Porter, C.W. Activated polyamine catabolism depletes acetyl-CoA and suppresses prostate tumor growth in the TRAMP mouse. J. Biol. Chem. 279:40076-40083, 2004. (see Appendix).
14. Greenberg, N.M., DeMayo, F., Finegold, M.J., Medina, D., Tilley, W.D., Aspinal, J.O., Cunha, G.R., Donjacour, A.A., Matusik, R.J., Rosen, J.M., Proc. Nat'l. Acad. Sci. USA 92:3439-43, 1995.
15. Pietilä, M., Alhonen, L., Halmekytö, M., Kanter, P., Jänne, J. and Porter, C.W., Activation of polyamine catabolism profoundly alters tissue polyamine pools and affects hair growth and female fertility in transgenic mice overexpressing spermidine/spermine N^1-acetyltransferase. J. Biol. Chem. 272:18746-18751, 1997.
16. Niiranen, K., Pietila, M., Pirttila, T.J., Jarvinen, A., Halmekyto, M., Korhonen, V.P., Alhonen, L., Janne, J. Targeted disruption of spermidine/spermine N1-acetyltrasferase gene in mouse embryonic stem cells. J. Biol. Chem. 277:25323-8, 2002.
17. Vujcic, S., Liang, P., Diegelman, P., Kramer, D.L. and Porter, C.W. Genomic identification and biochemical characterization of the mammalian polyamine oxidase involved in polyamine back-conversion. Biochem J. 370:19-28, 2003.
18. Vujcic, S., Diegelman, P., Bacchi, C.J., Kramer, D.L., and Porter, C.W., Identification and characterization of a novel flavin-containing spermine oxidase of mammalian cell origin. Biochem. J. 367:665-675, 2002.
19. Chen, Y., Vujcic, S., Liang, P., Diegelman, P., Kramer, D., and Porter, C.W. Genomic identification and biochemical characterization of a second spermidine/spermine N^1-acetyltransferase. Biochem J. (Accelerated Pub) 373:661-667, 2003.

DAMD17-03-1-0024

APPENDIX 1

FIGURES

&

REPRINTS

- Kee, K., Vujcic, S., Merali, S., Diegelman, P., Kisiel, N., Powell, C.T., Kramer, D.L. and Porter, C.W. Metabolic and antiproliferative consequences of activated polyamine catabolism in LNCaP prostate carcinoma cells. J. Biol. Chem. 279:27050-27058, 2004.
- Kee, K., Foster, B.A., Merali, S., Vujcic, S.,, Mazurchuk, R., Hensen, M.L., Diegelman, P., Kisiel, N., Kramer, D.L., and Porter, C.W. Activated polyamine catabolism depletes acetyl-CoA and suppresses prostate tumor growth in the TRAMP mouse. J. Biol. Chem. 279:40076-40083, 2004.

Figure 1

Figure 1. Metabolic ratchet model for polyamine homeostasis. Large arrows represent the primary pathways for polyamine biosynthesis (left) and catabolism (right). Various metabolites are shown which are either substrates or products of these pathways. Substrates and precursors utilized in polyamine biosynthesis include ornithine (Orn), methionine (Met) and the SAMDC aminopropyl donor, S-adenosylmethionine (SAM) while substrates utilized in polyamine catabolism include Spd, Spm, acetyl-CoA (AcCoA), and FAD. Compounds produced during polyamine biosynthesis include the natural polyamines (PA's), the SAMDC by-product decarboxylated S-adenosylmethionine (dcSAM), the Spd and Spm synthase by-product, methylthioadenosine (MTA) and the decarboxylase by-product, CO_2. Compounds produced during catabolism include the PAO product putrescine (Put) and the by-products hydrogen peroxide (H_2O_2), the aliphatic aldehyde 3-acetamidopropanal (RCHO's), and $FADH_2$. In response to SSAT-induced decreases in Spd and Spm, polyamine biosynthesis increases, giving rise to a sustained rise in metabolic flux. As flux through the pathway increases (such as that occurring in SSAT-tg mice), substrate utilization and product accumulation increase; conversely, as flux decreases (such as that occurring in SSAT-ko mice), substrate utilization and product accumulation decrease. The cellular response to alterations in flux depend upon the particular metabolites that change and how effectively the cell can react to that change.

Figure 2

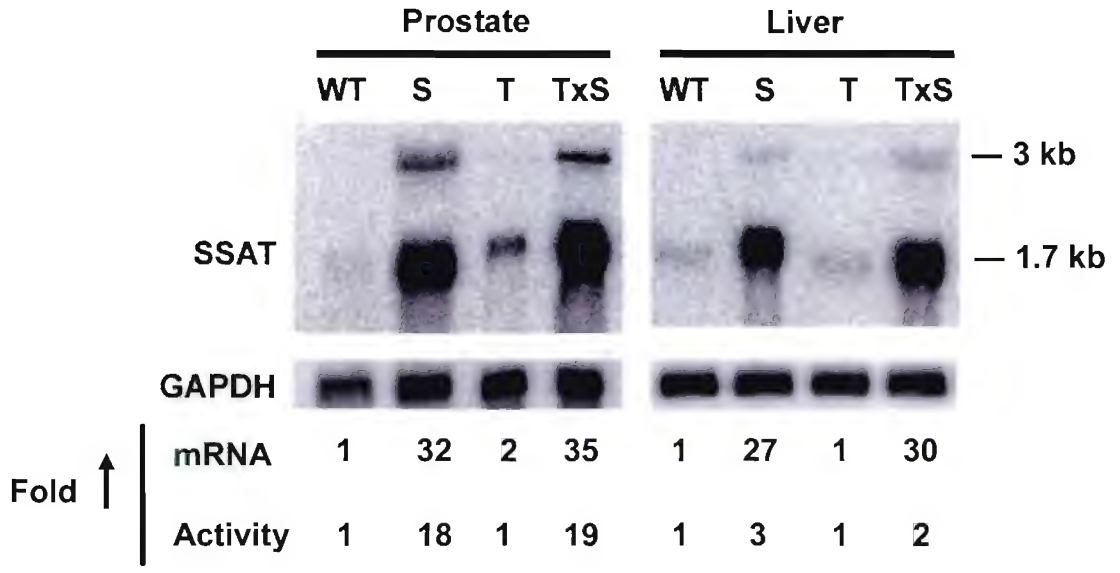

Figure 2. SSAT expression in the prostates and livers from SSAT transgenic mice. Total RNA was isolated from the prostates and livers of littermates obtained from the TRAMP x SSAT cross and subjected to Northern blot analysis and enzyme activity assay (33,39). Note the presence of a 3 kb heteronuclear SSAT RNA and a 1.7 kb mature SSAT mRNA. For quantitation, the 1.7 kb SSAT mRNA bands were scanned densitometrically and normalized to the glyceraldehyde-3'-phosphate dehydrogenase (GAPDH) signal. Both SSAT mRNA and activity were expressed as fold increase (Fold ↑) of wild-type tissue. SSAT mRNA was highly expressed in both prostate and liver of the SSAT (S) and the bigenic TRAMP/SSAT (TxS) mice but poorly expressed in the wild-type (WT) and TRAMP (T) animals. Northern blots are representative of those obtained during two experiments using 30 μg of total RNA/lane.

Figure 3

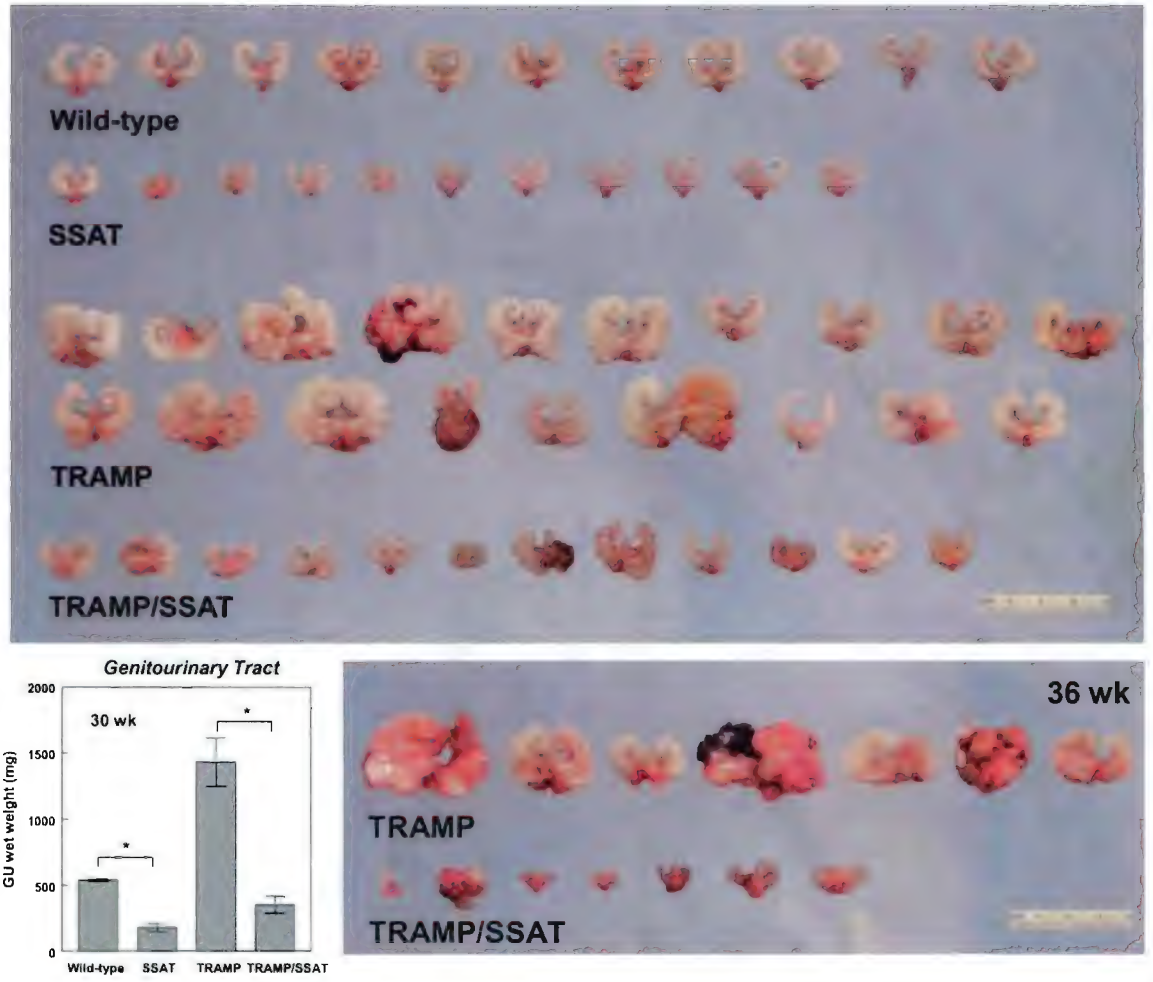

Figure 3. Comparison of GU tracts. (A) GU tracts of the four genetic cohorts deriving from the TRAMP x SSAT cross at 30 wk. Note that the GU tracts of SSAT mice were smaller than those of wild-type mice and that the GU tracts of TRAMP/SSAT mice were much smaller and less variable in size and shape than those of TRAMP mice. (B) GU tract weights at 30-wk of four genetic cohorts deriving from the TRAMP x SSAT cross. The GU tracts of TRAMP/SSAT animals weighed less than TRAMP mice (*$p < 0.0001$), and GU tracts of SSAT mice were also different from wild-type (*$p < 0.0001$) as determined by Student's unpaired t-test. (C) Comparison of GU tracts for TRAMP and TRAMP/SSAT mice at 36 wk of age. During the period 30 to 36 wk period, the average TRAMP GU tract increased by 200% while the average TRAMP/SSAT GU tract remained statistically the same.

Figure 4

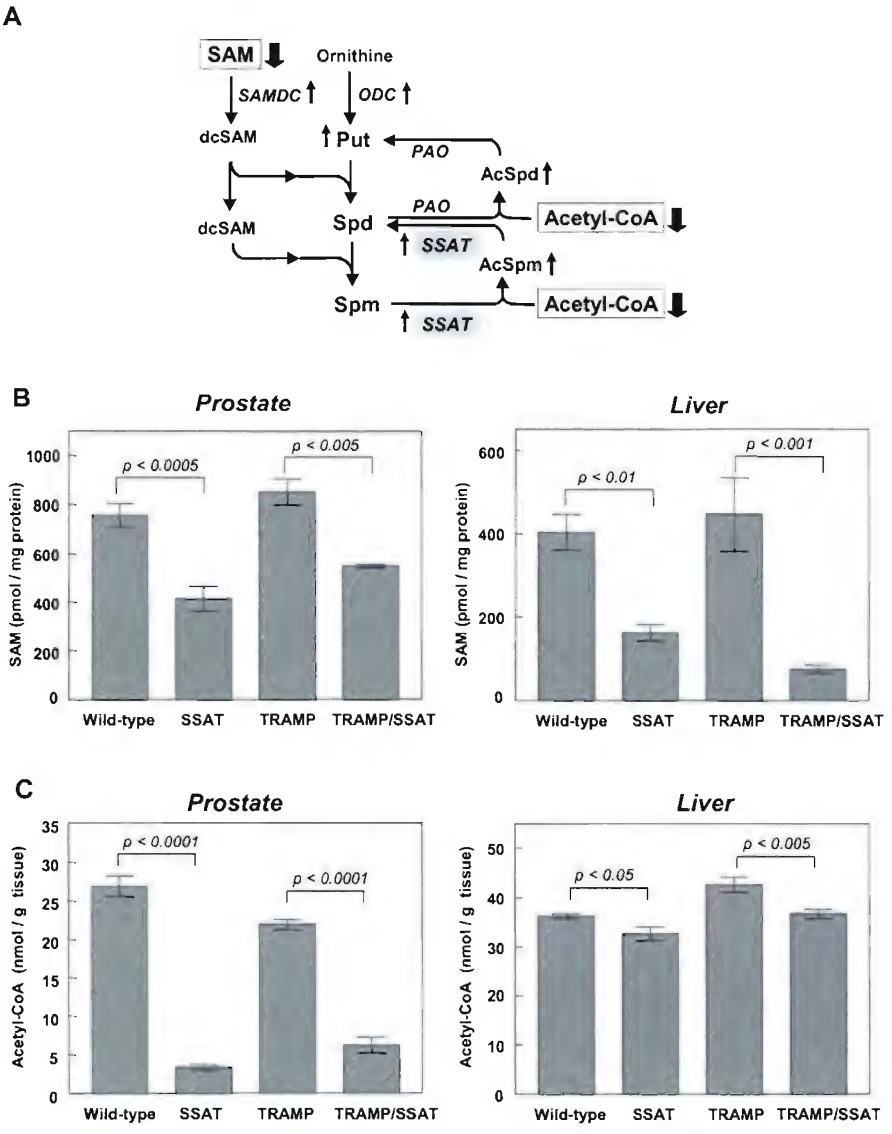

Figure 4. Downstream effects of SSAT overexpression. (A) Metabolic consequences to SSAT overexpression. Activation of polyamine catabolism at the level of SSAT results in a compensatory increase in the activities of the polyamine biosynthetic enzymes ODC and SAMDC. This activated polyamine synthesis minimizes polyamine pool depletion despite massive production of AcSpd. At the same time, it gives rise to heightened metabolic flux through the biosynthetic and catabolic pathways (not shown). The possible downstream consequences connecting heightened metabolic flux to growth inhibition include over-production of pathway products such as Put and AcSpd and/or depletion of critical metabolic precursors such as the aminopropyl donor SAM and the SSAT cofactor acetyl-CoA, both of which are markedly decreased in SSAT transgenic and TRAMP/SSAT bigenic animals. (B) SAM levels in prostate and liver tissues of TRAMP/SSAT littermates as determined on tissue extracts by HPLC. Note that SAM pools were much lower (>40%) in the prostate and liver of SSAT and TRAMP/SSAT mice. (C) Acetyl-CoA levels in prostate and liver tissues of TRAMP x SSAT littermates as

detected by HPCE. Note that during SSAT overexpression, there was significant reduction (~70%) of acetyl-CoA in the prostates of SSAT and TRAMP/SSAT mice but not in the livers. Data represents mean ± standard error, where n = 3 animals per group. Statistical significance (*p*-value) was determined by ANOVA with Fisher's PLSD test for pair-wise comparisons.

Figure 5

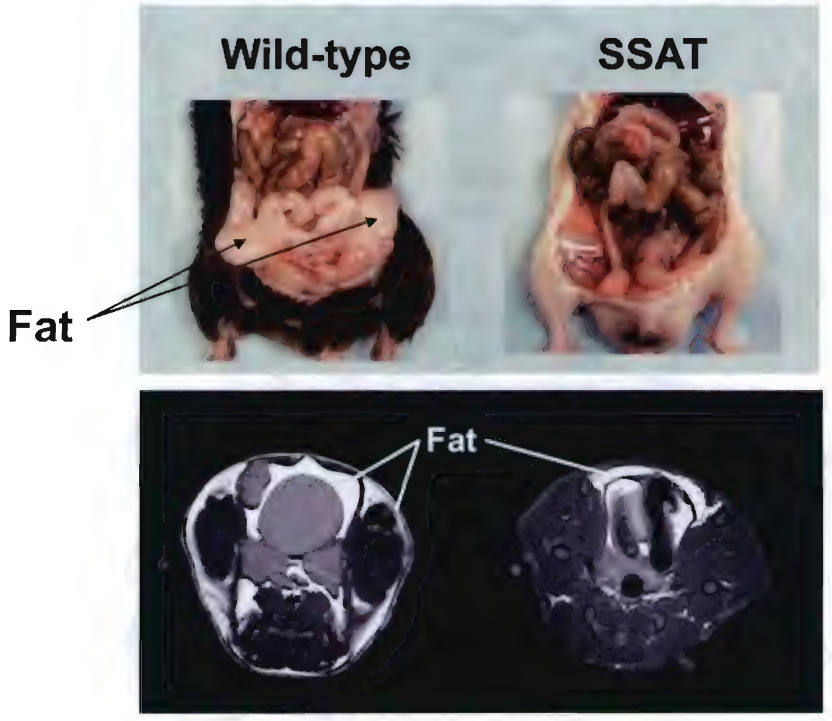

Figure 5. Abdominal fat stores in wild-type and SSAT transgenic mice at 30 wk. A Comparison of dissected mice (upper panel) shows the presence of large abdominal/mesenteric fat deposits in wild-type animals (left) and the absence of similar deposits in the SSAT transgenic animals (right). Representative high resolution transaxial MR images (lower panels) of wild type (left) and SSAT (right) mice. Note the presence of abdominal and sub-dermal fat (seen as bright areas) in wild-type mice and the absence of similar deposits in SSAT transgenic mice.

Figure 6

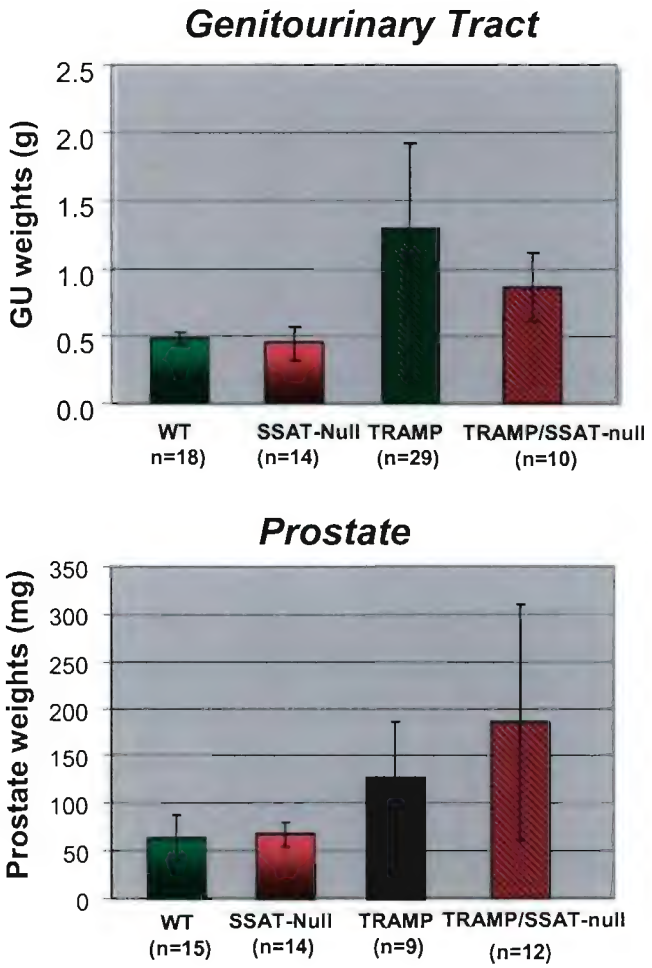

Figure 6. Effect of SSAT deletion on prostatic tumorigenesis in the TRAMP mouse. TRAMP mice were cross bred with SSAT null mice (both in the C57 Bl/6 background). Prostate glands and genitourinary tract (GU) weights were obtained at 30 wks. Observations thus far suggest that in both TRAMP and TRAMP/SSAT null, tumors originate in the prostate and rapidly spread to the seminal vesicles (as per GU weights). Note the difference in scale for the two tissues. Thus, the majority of the GU weight derives from the prostate and the difference between the two mouse cohorts was not found to be significant ($p < 0.05$). Additional mice are being accumulated for these studies.

Figure 7

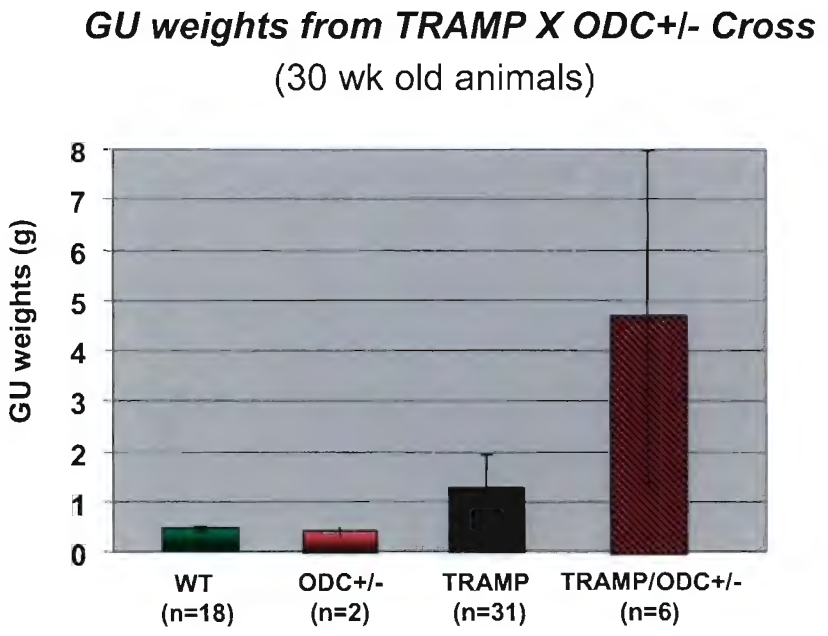

Figure 7. Effect of ODC haploinsufficiency on prostatic tumorigenesis in the TRAMP mouse. *TRAMP* mice were cross bred with heterozygous ODC mice (both in the C57 Bl/6 background). Genitourinary tract (GU) weights were obtained at 30 wks. Unlike TRAMP mice that typically show tumor invasion of the seminal vesicles, the majority of the TRAMP/ODC+/- tumors remained confined to the prostate. Despite large variation in tumor size, there is clear indication among individual animals that ODC heterogeneity promotes tumorigenesis within the prostate gland. Additional animals will be analyzed during the next year in order to counter the experimental variability.

Figure 8

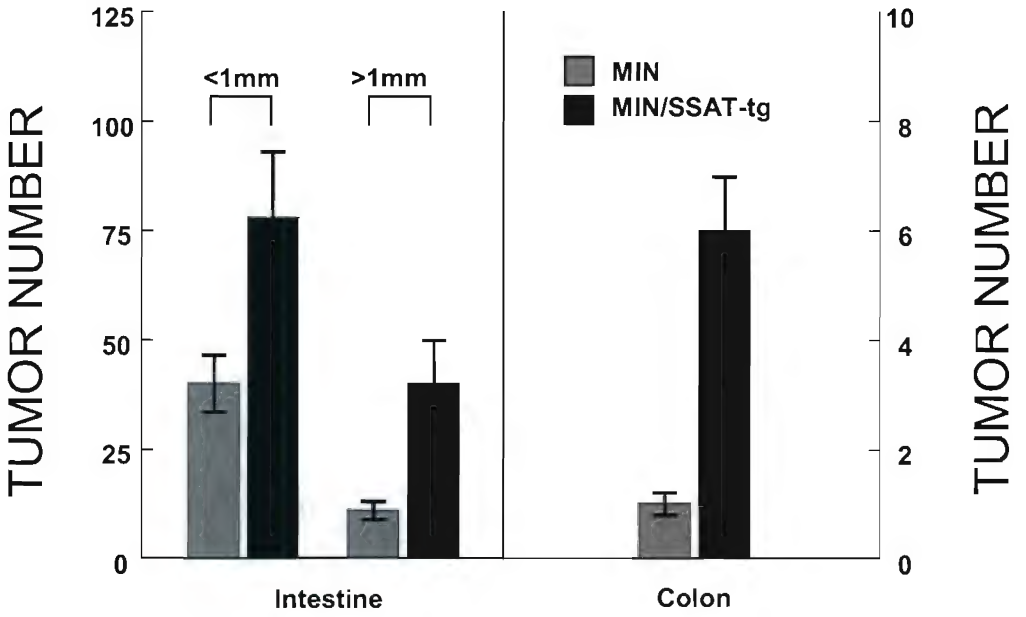

Figure 8. Effect of SSAT overexpression on intestinal tumorigenesis. *APC^{min}* mice were crossed with SSAT transgenic mice (both in the C57 Bl/6 background). Tumor counts at 40 days obtained from *APC^{min}* (n = 14) and *APC^{min}* x SSAT transgenic (n = 16) mice were determined on the entire length of small intestine and colon. For the small intestine, tumors <1 mm in diameter and those >1 mm in diameter were counted separately (designated above the bars). All tumors arising in the colon were >1 mm. *Note that SSAT expression markedly increased the number of tumors in both the intestine and the colon relative to the APC^{min} mice..*

JOURNAL OF BIOLOGICAL CHEMISTRY
Vol. 279, No. 26, Issue of June 25, pp. 27050–27058, 2004

Printed in U.S.A.

etabolic and Antiproliferative Consequences of Activated olyamine Catabolism in LNCaP Prostate Carcinoma Cells*

Received for publication, March 25, 2004, and in revised form, April 9, 2004
Published, JBC Papers in Press, April 19, 2004, DOI 10.1074/jbc.M403323200

Kristin Kee‡, Slavoljub Vujcic‡, Salim Merali§, Paula Diegelman‡, Nicholas Kisiel‡, C. Thomas Powell¶, Debora L. Kramer‡, and Carl W. Porter‡‖

From the ‡Grace Cancer Drug Center, Roswell Park Cancer Institute, Buffalo, New York 14263, the §Department of Medical and Molecular Parasitology, New York University School of Medicine, New York, New York 10010, and the ¶Cleveland Clinic Foundation, Lerner Research Institute, Cleveland, Ohio 44195

Depletion of intracellular polyamine pools invariably inhibits cell growth. Although this is usually accomplished by inhibiting polyamine biosynthesis, we reasoned that this might be more effectively achieved by activation of polyamine catabolism at the level of spermidine/spermine N^1-acetyltransferase (SSAT); a strategy first validated in MCF-7 breast carcinoma cells. We now examine the possibility that, due to unique aspects of polyamine homeostasis in the prostate gland, tumor cells derived from it may be particularly sensitive to activated polyamine catabolism. Thus, SSAT was conditionally overexpressed in LNCaP prostate carcinoma cells via a tetracycline-regulatable (Tet-off) system. Tetracycline removal resulted in a rapid ~10-fold increase in SSAT mRNA and an increase of ~20-fold in enzyme activity. SSAT products N^1-acetylspermidine, N^1-acetylspermine, and N^1,N^{12}-diacetylspermine accumulated intracellularly and extracellularly. SSAT induction also led to a growth inhibition that was not accompanied by polyamine pool depletion as it was in MCF-7 cells. Rather, intracellular spermidine and spermine pools were maintained at or above control levels by a robust compensatory increase in ornithine decarboxylase and *S*-adenosylmethionine decarboxylase activities. This, in turn, gave rise to a high rate of metabolic flux through both the biosynthetic and catabolic arms of polyamine metabolism. Treatment with the biosynthesis inhibitor α-difluoromethylornithine during tetracycline removal interrupted flux and prevented growth inhibition. Thus, flux-induced growth inhibition appears to derive from overaccumulation of metabolic products and/or from depletion of metabolic precursors. Metabolic effects that were not excluded as possible contributing factors include high levels of putrescine and acetylated polyamines, a 50% reduction in *S*-adenosylmethionine, and a 45% decline in the SSAT cofactor acetyl-CoA. Overall, the study demonstrates that activation of polyamine catabolism in LNCaP cells elicits a compensatory increase in polyamine biosynthesis and downstream metabolic events that culminate in growth inhibition.

Cell growth is dependent on a sustained supply of polyamines, which is typically met by the integrated contributions of biosynthesis, catabolism, uptake, and export, each of which is sensitively regulated by effector molecules that, in turn, are controlled by intracellular polyamine pools (1). Thus, ornithine decarboxylase (ODC)[1] and *S*-adenosylmethionine decarboxylase (SAMDC) control biosynthesis, a polyamine transport system modulates uptake, and spermidine/spermine N^1-acetyltransferase (SSAT) regulates polyamine catabolism and export out of the cell. Neoplastic cell growth is associated with elevated polyamine biosynthetic activity, even when the surrounding normal tissue itself is rapidly proliferating, such as the intestinal mucosa (2–4). Thus, the rationale for targeting polyamines in antitumor strategies relates to their critical role in supporting neoplastic cell growth and to the overexpression of biosynthetic enzymes in tumor *versus* normal tissues (3, 5, 6).

The biology and metabolism of polyamines in the prostate is distinctly different from that of other tissues. In addition to synthesizing these molecules for epithelial cell replacement, the gland produces massive quantities of spermine (Spm) for export into reproductive fluids (7–10). The only major tissue that synthesizes polyamines for export, the prostate, and presumably tumors derived from it, may be dependent on novel and therapeutically exploitable homeostatic mechanisms. For example, we have observed that, in contrast to other cell lines, two of three prostate carcinoma lines failed to regulate polyamine transport in response to polyamine analogues or inhibitors (11). Very recently, Rhodes *et al.* (12) performed a meta-analysis of four independent microarray datasets comparing gene expression profiles of benign *versus* malignant patient prostate samples (12). Their study showed that polyamine biosynthesis was the most consistently and significantly affected metabolic, signaling, or apoptotic pathway. More particularly, the study revealed a synchronous network of genes contributing to polyamine biosynthesis was up-regulated while genes detracting from polyamine biosynthesis were down-regulated. In support of these findings, clinical studies by Bettuzzi *et al.* (13) indicate a significant increase in transcripts of the polyamine biosynthetic enzymes, ODC and SAMDC, in human prostatic cancer relative to benign hyperplasia.

* This work was supported by NCI National Institutes of Health Grants CA-72648, CA-22153, CA-09072-30 and CA-16056 and by Department of Defense Award PC020638. The costs of publication of this article were defrayed in part by the payment of page charges. This article must therefore be hereby marked "*advertisement*" in accordance with 18 U.S.C. Section 1734 solely to indicate this fact.

‖ To whom correspondence should be addressed. Tel.: 716-845-3002; Fax: 716-845-2353; E-mail: carl.porter@roswellpark.org.

[1] The abbreviations used are: ODC, ornithine decarboxylase; CoA, coenzyme A; AcSpd, N^1-acetylspermidine; AcSpm, N^1-acetylspermine; dcSAM, decarboxylated *S*-adenosylmethionine, DiAcSpm, N^1,N^{12}-diacetylspermine; DENSPM, N^1,N^{11}-diethylnorspermine; DFMO, α-difluoromethylornithine; HPCE, high performance capillary electrophoresis; HPLC, high performance liquid chromatography; MTA, 5′-methylthioadenosine; PAO, polyamine oxidase; Put, putrescine; SAM, *S*-adenosylmethionine; SAMDC, *S*-adenosylmethionine decarboxylase; Spd, spermidine; Spm, spermine; SSAT, spermidine/spermine N^1-acetyltransferase; Tet, tetracycline; TRAMP, transgenic adenocarcinoma of mouse prostate; tTA, tetracycline-repressible transactivator; dansyl, 5-dimethylaminona-phthalene-1-sulfonyl.

In recognition of the unique physiology of the prostate gland, Heston and collaborators (14, 15) were among the first to propose that targeting polyamine biosynthesis may be particularly effective against prostate cancer. Most of these efforts have made use of known inhibitors of ODC or SAMDC (16–19). Gupta *et al.* (20) showed that the ODC inhibitor, α-difluoromethylornithine (DFMO) effectively suppressed development of prostate cancer in the TRAMP mouse model. As an alternative approach to the use of enzyme inhibition, we propose that disruption of polyamine homeostasis at the level of polyamine catabolism may have unique therapeutic potential against prostate carcinoma. It has been demonstrated, for example, that polyamine analogues such as N^1,N^{11}-diethylnorspermine (DENSPM) down-regulate polyamine biosynthesis at the level of ODC and SAMDC and, at the same time, potently (*i.e.* >200-fold) up-regulate polyamine catabolism at the level of spermidine/spermine N^1-acetyltransferase (SSAT) (1, 21–27). Several lines of evidence support the idea that analogue induction of SSAT and hence, activation of polyamine catabolism, is a critical determinant of DENSPM drug action. For example, DENSPM growth inhibition among tumor cell lines correlates with the extent to which SSAT is induced (23–25), and analogues that differentially induce SSAT inhibit cell growth in a correlative manner (22, 26, 27). As more direct evidence for this relationship, McCloskey *et al.* (28) showed that DENSPM-resistant Chinese hamster ovary cells are unable to induce SSAT. Recently, Chen *et al.* (29, 30) reported that small interference RNA interference with DENSPM induction of SSAT prevented polyamine pool depletion while blocking analogue-induced apoptosis in human melanoma cells.

The studies cited above relate to SSAT induction in the context of analogue treatment, but they do not address what happens when SSAT is selectively induced in cells. In an earlier report (31), we showed that conditional overexpression of SSAT leads to polyamine pool depletion and growth inhibition in MCF-7 breast carcinoma cells. On the basis of rationale suggesting that prostate carcinoma may react differently to perturbations in polyamine homeostasis, we investigated the consequences of conditional SSAT overexpression in LNCaP prostate carcinoma cells.

EXPERIMENTAL PROCEDURES

Materials—The inhibitor of polyamine oxidase (PAO), N^1-methyl-N^2-(2,3-butadienyl)butane-1,4-diamine (MDL-72527) was generously provided by Aventis Pharmaceuticals Inc. (Bridgewater, NJ). The ODC inhibitor DFMO was obtained from Ilex, Inc. (San Antonio, TX). Tetracycline (Tet), aminoguanidine, polyamines, and the acetylated polyamines N^1-acetylspermidine (AcSpd) and N^1-acetylspermine (AcSpm) were purchased from Sigma-Aldrich, whereas N^1,N^{12}-diacetylspermine (DiAcSpm) was provided as a gift from Dr. Nikolaus Seiler (Laboratory of Nutritional Oncology, Institut de Recherche Contre les Cancers, Strasbourg, France). SAM was purchased from Sigma-Aldrich, and the SAM metabolites, decarboxylated *S*-adenosylmethionine (dcSAM) and 5-methylthioadenosine (MTA), were synthesized and kindly provided by Drs. Canio Marasco and Janice Sufrin (Roswell Park Cancer Institute). Radioactive compounds L-[1-^{14}C]ornithine, [acetyl-1-^{14}C] coenzyme A, [α-^{32}P]dCTP were purchased from PerkinElmer Life Sciences, and *S*-adenosyl-L-[*carboxyl*-^{14}C]methionine was obtained Amersham Biosciences. Acetyl-coenzyme A (acetyl-CoA) was purchased from Sigma-Aldrich and solubilized as described by Liu *et al.* (32). Geneticin (G418) and hygromycin B were obtained from Clontech Laboratories, Inc. (Palo Alto, CA) and Invitrogen, respectively.

Cell Culture—LNCaP prostate carcinoma cells engineered to constitutively express the tetracycline-repressible transactivator (tTA) (33), designated LNGK9 (34), were cultured in RPMI 1640 media supplemented with 2 mM glutamine (Invitrogen), 10% Tet-approved fetal bovine serum (Clontech Laboratories, Inc.), penicillin at 100 units/ml, streptomycin at 100 units/ml (Invitrogen), and 150 μg/ml hygromycin B at 37 °C in the presence of humidified 5% CO_2. Aminoguanidine (at 1 mM) was routinely included in the media as an inhibitor of copper-dependent bovine serum amino oxidases to prevent conversion of extracellular polyamines to toxic products. Cells were harvested by trypsinization and counted electronically (Coulter Model ZM, Coulter Electronics, Hialeah, FL).

Transfections—LNGK9 cells expressing the tTA were seeded at 2 × 10^6 cells per 100-mm culture dishes in the absence of hygromycin B and Tet. The following day, fresh media were replaced and cells were co-transfected with the tTA-responsive pTRE-SSAT plasmid (31) and a G418-resistance selection plasmid pcDNA3 (Invitrogen) at a ratio of 20:1 using FuGENE 6 (Roche Applied Science) according to manufacturer's protocol. Stably transfected clones were selected in medium containing 500 μg/ml antibiotic G418, 150 μg/ml hygromycin B, and 1 μg/ml Tet. Healthy G418-resistant clones were selected and tested for SSAT mRNA by Northern blot analysis in the presence or absence of 1 μg/ml Tet. With the Tet-off system, SSAT transcription is induced in the absence of Tet (−Tet) but not in its presence (+Tet). A Tet concentration of 1 μg/ml was found to fully and consistently suppress SSAT gene expression during routine cell culture passage. Clones that expressed low basal level of SSAT mRNA under +Tet conditions and high induced levels of SSAT mRNA under −Tet conditions were selected for further study. Clones were maintained continuously under 1 μg/ml +Tet until experiments were initiated.

Northern Blot Analysis—Northern blot analysis was carried out as described by Fogel-Petrovic *et al.* (35) with modifications. Briefly, total RNA was extracted with an RNeasy® Mini kit (Qiagen Inc., Valencia, CA), and its concentration was determined by UV spectrophotometry. RNA samples (5 μg/lane) were separated on 1.5% agarose/formaldehyde gels and transferred to a Duralon-UV membrane (Stratagene, La Jolla, CA). The membrane was cross-linked in a Stratalinker™ 1800, hybridized to [^{32}P]dCTP random-labeled cDNA probes (Stratagene) for detection of SSAT mRNA (36), and exposed for autoradiography. A glyceraldehyde-3-phosphate dehydrogenase signal was used as a loading control.

Polyamine Enzymes and Polyamine Pools—SSAT, ODC, and SAMDC activities were assayed as described previously (27, 37). Polyamine enzyme activities were expressed as picomoles of AcSpd generated per minute/mg of protein for SSAT and as nanomoles of CO_2/h/mg of protein for ODC and SAMDC. Intracellular polyamines, including acetylated derivatives of spermidine (Spd) and Spm were extracted from cell pellets with 0.6 N perchloric acid, dansylated, measured by reverse phase high-performance liquid chromatography (HPLC) as described by Kramer *et al.* (38), and expressed as picomoles/10^6 cells. Extracellular polyamines and acetylated polyamines were extracted from media as described by Kramer *et al.* (39), containing fetal bovine serum, Tet, and L-glutamine but not G418 or hygromycin B. A total of 50 μl of dansylated sample was injected for HPLC, and data were collected and analyzed as noted above. Extracellular polyamine pools were expressed as nanomoles/equivalent volume (ml)/10^6 cells.

S-Adenosylmethionine and Metabolite Pools—Intracellular SAM and its metabolites, dcSAM and MTA, were extracted from cell pellets with 0.6 N perchloric acid and measured by HPLC according to chromatographic conditions reported by Yarlett and Bacchi (40) with modifications as described by Kramer *et al.* (38). Briefly, samples (50 μl) were eluted from a C18 column (40 °C) at a flow rate of 0.8 ml/min with a linear gradient starting with solvent A (0.1 M NaH_2PO_4, 8 mM octane sulfonic acid, 0.05 mM EDTA, 2% acetonitrile) at 80% and solvent B (0.15 mM NaH_2PO_4, 8 mM octane sulfonic acid, 26% acetonitrile) at 20%. Over the course of 30 min, the gradient increased to 100% solvent B for 10 min. Effluent was monitored with a Waters 2487 dual wavelength UV detector, and data were processed using instrumentation described for polyamine pool analysis and expressed as picomoles/10^6 cells.

Measurement of Acetyl-CoA—High performance capillary electrophoresis (HPCE) separation and quantitation of acetyl-CoA in biological samples followed the method of Liu *et al.* (32). Cells were lysed and processed by using a solid-phase extraction. Extracts were then analyzed on a Beckman P/ACE MDQ capillary electrophoresis system equipped with a photodiode array detector and an uncoated fused silica CE column of 75-μm inner diameter and 60 cm in length with 50 cm from inlet to the detection window (Polymicro Technologies, Phoenix, AZ). Electrophoretic conditions were according to Liu *et al.* (32) with modifications. Briefly, the capillary was preconditioned with 1 M NaOH and Milli-Q water for 10 min each at 20 p.s.i. and then equilibrated with 100 mM NaH_2PO_4 running buffer containing 0.1% β-cyclodextrin (pH 6.0) for 10 min. After each run, the capillary was rinsed with 1 M NaOH, Milli-Q water, and running buffer for 2 min each. The injection was done hydrodynamically at a pressure of 0.5 p.s.i. for 10 s. Injection volume was calculated using CE Expert Lite software from Beckman. Separation voltage was 15 kV at a constant capillary temperature of 15 °C. To establish the standard calibration curves, solutions contain-

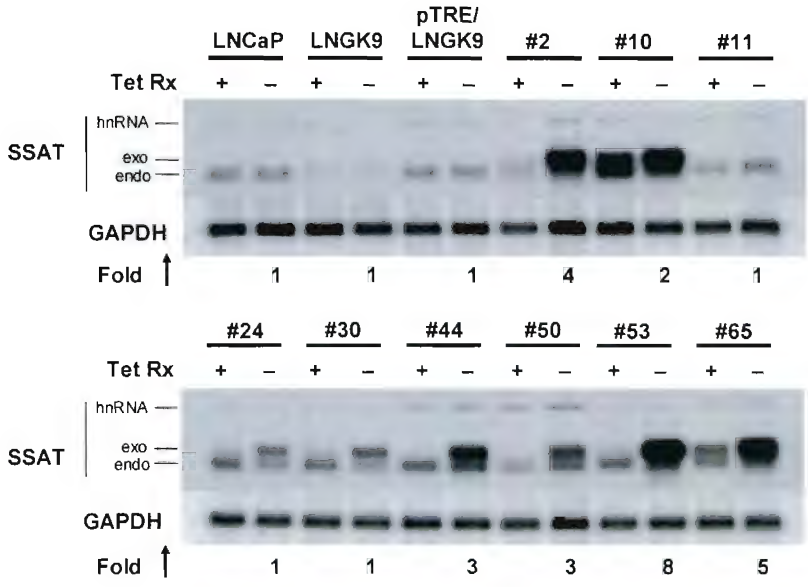

FIG. 1. **Conditional overexpression of SSAT mRNA in LNCaP clones transfected with Tet-regulatable human SSAT cDNA. LNGK9 cells, a subline of LNCaP, were transfected with the Tet-repressible human SSAT plasmid.** Stably transfected clones resistant to neomycin were selected and tested for their responsiveness to Tet by Northern blot analysis. Representative examples from over 100 selected clones were cultured for 48 h in the presence (+) or absence (−) of 1 μg/ml Tet. Note the endogenous (*endo*) and exogenous (*exo*, *i.e.* plasmid transcript) mature SSAT mRNA can be distinguished on the basis of size (*i.e.* ~1.3 *versus* ~1.5 kb, respectively). For quantitation, the exogenous and endogenous SSAT mRNA bands were scanned fluorometrically, normalized to the glyceraldehyde-3-phosphate dehydrogenase (*GAPDH*) signal, and expressed as -fold increase (*Fold* ↑) in −Tet relative to +Tet. Blots are representative of findings from three separate experiments. *hnRNA*, heteronuclear RNA.

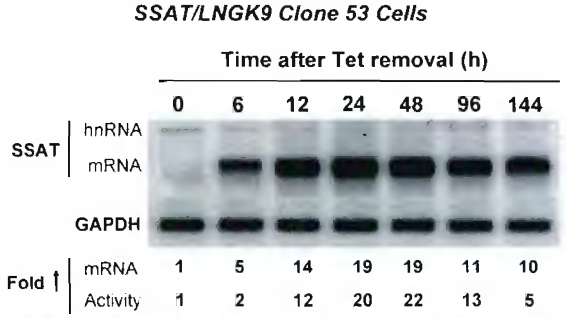

FIG. 2. **Time-dependent increases in SSAT mRNA and activity in SSAT/LNGK9 clone 53 following Tet removal.** Tet was removed for the indicated time, and cells were harvested for total RNA isolation and SSAT enzyme activity. An amount of 5 μg of total RNA was loaded onto each Northern blot lane. Note that following removal of 1 μg/ml Tet, both SSAT mRNA and activity increased rapidly before reaching a plateau between 24 and 48 h. For quantitation, SSAT mRNA bands were scanned fluorometrically, normalized to the glyceraldehyde-3-phosphate dehydrogenase (*GAPDH*) signal, and expressed as -fold increase (*Fold* ↑) relative to +Tet at 0 h (*lane 1*). As expressed by -fold increase, SSAT activity increased in parallel to SSAT mRNA. This blot is representative of findings from three separate experiments. *hnRNA*, heteronuclear RNA.

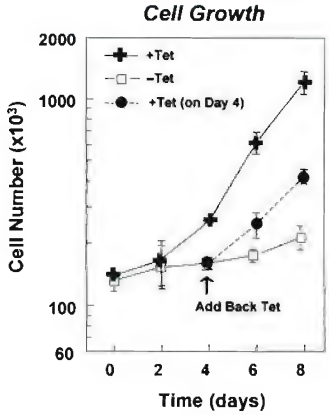

FIG. 3. **Effects of conditional SSAT overexpression on growth kinetics of LNCaP prostate carcinoma cells.** SSAT/LNGK9-clone 53 cells were cultured in the presence (+*Tet*, ✚) or absence (−*Tet*, □) of 1 μg/ml Tet for the indicated time and collected for growth analysis. Removal of Tet (□) resulted in an inhibition of cell growth over the course of 8 days. Note that addition of 1 μg/ml Tet at 96 h (●) leads to a resumption of cell growth. Data represent means ± S.E., where *n* is 3.

ing the acetyl-CoA and the internal standard (isobutyryl-CoA, 41 nmol) were prepared at concentrations ranging from 1 to 200 nmol. Standards were processed as described above for cell lysates and resuspended in 10 μl of water. The detector response was ($r > 0.99$) for all acetyl-CoA species over the above concentration range. Coenzyme As were monitored with a photodiode array detector at the maximum absorbance wavelength (253.5 nm). Data were collected and processed by using Beckman P/ACE 32 Karat software version 4.0. Cellular acetyl-CoA levels were expressed as nanomoles/10^6 cells.

RESULTS

Derivation of Transfected Cells—Cells transfected with the human SSAT cDNA were selected in neomycin and grown as clones in the presence of 1 μg/ml Tet. Of the 100 SSAT/LNGK9 clones screened (data not shown), those most sensitive to Tet regulation were selected according to the differential expression between SSAT mRNA in +Tet (SSAT-off) *versus* mRNA in −Tet (SSAT-on) (Fig. 1). Based on these criteria, clone 53 was selected for further study, because it displayed low SSAT mRNA in +Tet and an 8-fold increase in total SSAT mRNA (exogenous and endogenous) under −Tet conditions for 48 h. Nearly identical responses were also obtained with several other clones. Transfected human SSAT cDNA (~1.5 kb) was distinguishable from the smaller endogenous transcript (~1.3 kb) by differences in polyadenylation, which became apparent during enzyme induction (35). Although the exogenous 1.5-kb transcript levels increased with Tet removal, the endogenous 1.3-kb transcript levels remained at basal levels, indicating that the presence or absence of the antibiotic did not affect endogenous gene expression. Tet-regulated expression of SSAT mRNA and activity was characterized from 0 to 144 h in clone 53 (Fig. 2). Following Tet removal, SSAT mRNA increased significantly by 6 h and plateaued by 24 h at levels ranging between 10- and 20-fold greater than the 0-h sample. Induction of mRNA was closely paralleled by increases in SSAT activity, which reached a maximum of ~20-fold by 24 h (see Figs. 2 and 4).

Effects of SSAT Overexpression on Cell Growth and Polyamine Metabolism—As shown in Fig. 3, SSAT overexpression caused significant inhibition of cell growth at ~2 days following Tet removal, which was sustained through the 6-day experiment. Growth inhibition appeared to be cytostatic rather than cytotoxic, because there was no obvious decline in cell number as would be expected with apoptosis and because addition of

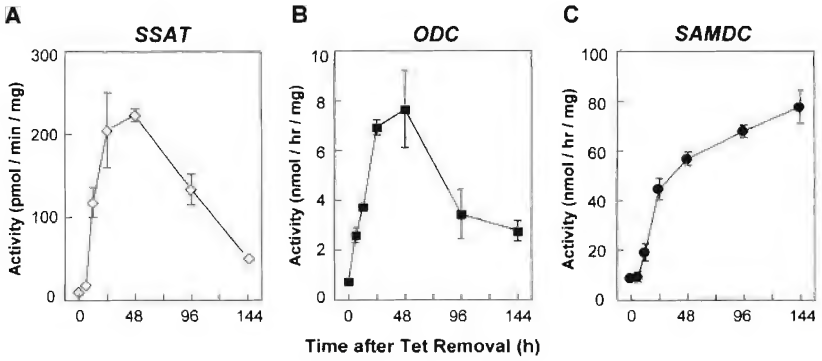

FIG. 4. **Time-dependent effects of conditional SSAT overexpression on polyamine biosynthetic enzyme activities.** Tet was removed from SSAT/LNGK9-clone 53 cells for the indicated time after which cells were harvested for polyamine enzyme activities for SSAT, ODC, and SAMDC. Following Tet removal, both SSAT activity (◇) increased sharply to a maximum of ~20-fold (*A*), and ODC activity (■) increased sharply to ~10-fold (*B*) at 48 h before undergoing a steady decline. By contrast, SAMDC activity (●) increased steadily over the course of 144 h to a maximum of ~18-fold that of basal levels (*C*). Enzyme activities of SSAT/LNGK9-clone 53 cells grown continuously in the presence of Tet remained relatively unchanged from 0 h (data not shown). Data represents mean values ± S.E., where *n* is 3.

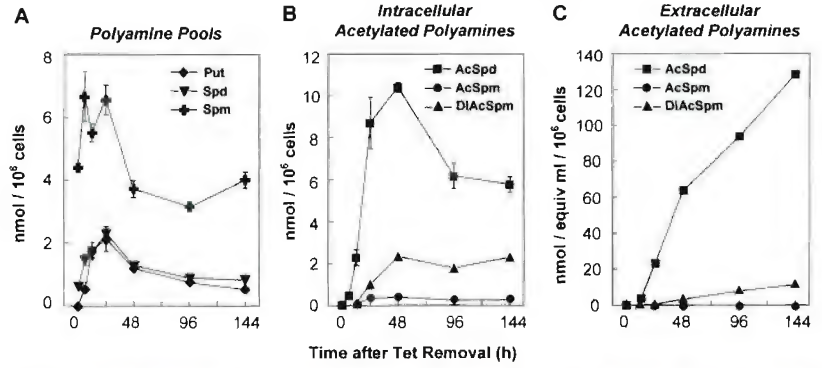

FIG. 5. **Time-dependent effects of conditional SSAT overexpression on intracellular and extracellular polyamines.** Similar to the experiment as described in Fig. 4, SSAT/LNGK9-clone 53 cells were grown in the absence of Tet for the indicated time and then harvested for polyamine pool analysis by HPLC. Intracellular polyamines pools increased transiently for 24 h following Tet removal and then decreased steadily. Note that, even at 144 h, Put, Spd, and Spm pools remained similar to or slightly above basal levels (0 h) (*A*). Intracellular AcSpd and AcSpm increased markedly following Tet removal (*B*). At the same time, huge amounts of AcSpd accumulated in the media (*C*) indicating that acetylated products are readily exported. Significant levels of DiAcSpm were detected intracellularly and extracellularly (*B* and *C*). (*AcSpd*, N^1-acetylspermidine; *AcSpm*, N^1-acetylspermine; *DiAcSpm*, N^1,N^{12}-diacetylspermine; *Put*, putrescine; *Spd*, spermidine; *Spm*, spermine). Data represent means ± S.E., where *n* is 3.

Tet at 96 h resulted in a rapid resumption of cell growth (Fig. 3). The time-dependent effects of Tet removal on enzyme activities and polyamine pools are shown in Figs. 4 and 5. SSAT increased steadily to 22-fold by 48 h before declining slowly from 48 to 144 h (Figs. 2 and 4). This steady decrease in SSAT activity and mRNA may be due to a homeostatic adjustment of gene expression and/or to a time-dependent selection of cells that express lower levels of SSAT. Consistent with the observed rise in enzyme activity, acetylated polyamines increased under −Tet conditions (Fig. 5). Intracellular AcSpd increased remarkably from undetectable levels (<10 pmol/10^6 cells) to 10,420 pmol/10^6 cells by 48 h. Other SSAT products, AcSpm and DiAcSpm, which are rarely seen in cells (31), accumulated to 390 pmol/10^6 cells and 2,340 pmol/10^6 cells, respectively, by 48 h and remained elevated during the course of the 144-h experiment. Putrescine (Put) pools also rose remarkably due presumably to back-conversion of Put from Spd via AcSpd (Fig. 5) and to forward synthesis due to increased ODC activity (described below). Despite the massive accumulation of acetylated polyamines, intracellular levels of Spd and Spm failed to decrease. In fact, the levels of Put, Spd, and Spm increased substantially during the first 24 h following SSAT induction, after which they declined slowly to levels that were above (*i.e.* Put and Spd) or close to (*i.e.* Spm) 0 h levels. Enzyme activity data in Fig. 4 (*B* and *C*) strongly suggest that these pools were sustained by compensatory increases in ODC and SAMDC activities, which rose ~10-fold and ~8-fold, respectively, during the first 48 h of SSAT overexpression (Fig. 4*A*).

Analysis of cell culture media revealed huge amounts of acetylated polyamines following SSAT overexpression (Fig. 5*C*). In particular, AcSpd and DiAcSpm, which were barely detectable in +Tet culture media, were as high as 128,210 pmol/equivalent ml/10^6 cells and 11,500 pmol/equivalent ml/10^6 cells, respectively, 144 h following Tet removal. These extracellular levels were actually 10-fold higher than intracellular levels on the basis of 10^6 cells. The finding is consistent with the tenet that acetylation by SSAT facilitates export of polyamines out of the cell (41–43). Taken together, the above findings indicate that SSAT induction leads to a strong metabolic flux through both the biosynthetic and catabolic arms of the polyamine pathway. As additional indication for this interpretation, we observed increased conversion of SAM to dcSAM via the SAMDC reaction and increased intracellular accumulation MTA, a well known by-product of dcSAM that is stoichiometrically released during the Spd and Spm synthase reactions (Fig. 6).

Effects of PAO and ODC Inhibition on SSAT-induced Growth Inhibition and Pool Dynamics—Data in Figs. 4 and 5 indicate that SSAT overexpression and inhibition of cell growth in LNCaP cells were *not* due to depletion of intracellular Spd and Spm pools. Thus, our next experiments were designed to investigate the basis for SSAT-induced growth inhibition in LNCaP

cells. Because polyamine oxidase (PAO) is functionally located downstream of SSAT, and because the enzyme liberates toxic by-products (hydrogen peroxide and reactive aldehydes) having clear cytotoxic potential (44), we first examined whether the PAO inhibitor MDL-72527 might prevent growth inhibition during SSAT-mediated deregulation of polyamine catabolism. As shown in Fig. 7*A*, the presence of 10 μM MDL-72527 during −Tet failed to abrogate growth inhibition. The substantial increase in acetylated polyamines during inhibitor treatment relative to −Tet alone confirms that PAO was effectively blocked (Table I). We next considered that growth inhibition might be due to metabolic flux resulting from up-regulation of ODC and polyamine biosynthesis. To test this hypothesis, the specific ODC inhibitor DFMO was added to the media during Tet removal to interrupt metabolic flux. As others have reported (45), wild-type LNCaP cells are inherently resistant to DFMO. SSAT-off (+Tet) cells treated with 1 mM DFMO grew similarly to cells not treated with DFMO (Fig. 7). The more unexpected finding was that DFMO treatment of SSAT-on (−Tet) cells effectively prevented growth inhibition. Thus, by inhibiting ODC, a relationship between metabolic flux and the antiproliferative effect was established. Importantly, ODC inhibition fully prevented accumulation of acetylated polyamines (Table I) and thereby provided direct evidence for interruption of polyamine flow from biosynthesis to catabolism. In experiments to be discussed below (see Fig. 10*D*), interference with flux by DFMO is further confirmed by the fact that there is no accumulation of MTA, the by-product of Spd and Spm synthesis.

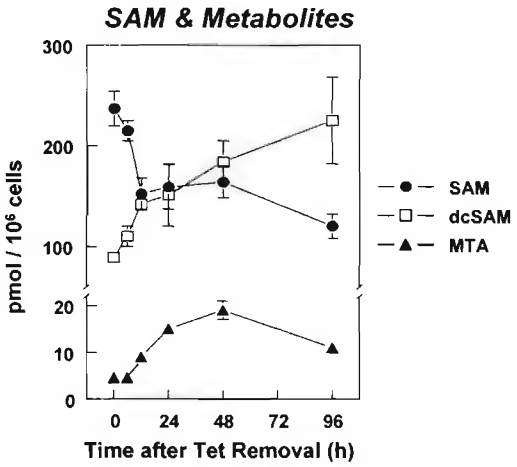

FIG. 6. **Effects of SSAT overexpression on SAM, dcSAM and MTA pools.** Tet was removed from SSAT/LNGK9-clone 53 cells for the indicated times after which cells were harvested and extracted for SAM pool analysis by HPLC. Note that upon Tet removal (−Tet), intracellular levels of the SAMDC substrate SAM (●) declined steadily to ~50% at 96 h while the SAMDC product dcSAM (□) increased steadily to a maximum of 250% at 96 h. At the same time, the biosynthetic by-product of dcSAM metabolism MTA (▲) increased to a maximum of ~400% at 48 h. The findings are consistent with accelerated polyamine metabolic flux due to increased polyamine biosynthesis and acetylation in −Tet cells. The limit of detection for MTA is <5 pmol/10^6 cells. Data represent means ± S.E., where *n* is 3.

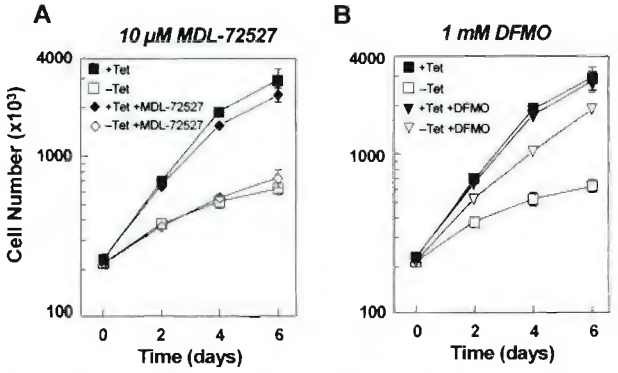

FIG. 7. **Effects of PAO or ODC inhibition on SSAT-induced cell growth inhibition.** SSAT/LNGK9-clone 53 cells were grown in the presence and absence of Tet and treated with either a PAO inhibitor (10 μM MDL-72527 (*A*)) or an ODC inhibitor (1 mM DFMO (*B*)) for the indicated time and then analyzed for prevention of cell growth inhibition. When included during Tet removal, the PAO inhibitor MDL-72527 failed to prevent growth inhibition by SSAT (*A*), whereas the ODC inhibitor DFMO was very effective in preventing SSAT-induced growth inhibition (*B*). Data represent means ± S.E., where *n* is 3.

The basis for sustained cell growth in the presence of DFMO is not clear by the polyamine analysis shown in Table I. At 48 h, Put and Spd pools are very low and Spm pools remain as high as those seen in the growth-inhibited −Tet cells. It is possible that, although most cells seem to rely on Spd for cell growth (18), LNCaP cells may grow under conditions of severe Put and Spd limitation by relying on Spm pools and a small amount of Spd back-converted from Spm via the SSAT/PAO pathway. Consistent with this idea, Spm pools were maintained at near to control levels for more than 96 h (data not shown).

Metabolic Flux and Depletion of Polyamine Precursor Stores—Enhanced metabolic flux may deplete metabolites and polyamine precursors and thereby limit their availability for cell growth. Such molecules include the biosynthetic precursors ornithine, methionine, SAM, and the SSAT cofactor acetyl-CoA. As shown in Fig. 8, the inclusion of 1 mM ornithine or methionine in the −Tet media failed to prevent SSAT-induced growth inhibition indicating that the amino acids were not limiting to cell growth.

The impact of SSAT overexpression on acetyl-CoA pools was investigated, because, in addition to serving as a cofactor to SSAT, the molecule is critically involved in fatty acid synthesis, histone acetylation, and other metabolic processes that could affect cell growth. As shown by electropherogram (Fig. 9*A*), acetyl-CoA was detectable by HPCE as a distinct and highly reproducible peak. Peak changes under −Tet *versus* +Tet conditions were quantitated relative to the internal standard

TABLE I
Polyamine pools under conditions of SSAT overexpression and enzyme inhibition in LNCaP cells

SSAT/LNGK9 clone 53	48-h treatment[a]	Polyamine pools (cells)[b]					
		Put	AcSpd	Spd	AcSpm	DiAcSpm	Spm
		pmol/10⁶cells					
+Tet	Untreated	<10	<10	685 ± 10	<10	<10	4,180 ± 102
−Tet	Untreated	960 ± 25	16,910 ± 623	885 ± 70	525 ± 20	5,300 ± 320	3,050 ± 147
+Tet	1 mM DFMO	<10	<10	40 ± 2	<10	<10	3,850 ± 88
−Tet	1 mM DFMO	<10	320 ± 80	90 ± 15	40 ± 3	<10	3,455 ± 373
+Tet	10 μM MDL-72527	215 ± 15	<10	1,135 ± 68	<10	<10	4,390 ± 328
−Tet	10 μM MDL-72527	985 ± 160	21,795 ± 852	1,110 ± 57	1,030 ± 55	8,765 ± 345	2,625 ± 179

[a] Treatment began at Tet removal.
[b] Data are expressed as means ± S.E., where *n* is 3.

isobutyryl-CoA. Following analysis, intracellular acetyl-CoA pools were found to decrease by ~25% at 48 h and by ~45% at 96 h (Fig. 9*B*) suggesting a cause-and-effect linkage. The inability of acetyl-CoA to penetrate cells precluded more defining prevention studies such as those involving amino acids (Fig. 8). Attempts to prevent growth inhibition with exogenous 1 mM pyruvate as an acetyl-CoA precursor, proved unsuccessful (data not shown). It is puzzling, however, that these pools were not protected during DFMO prevention of growth inhibition (Fig. 10*A*). Because inhibition of ODC by DFMO results in a marked increase in SAMDC activity and dcSAM pools (Fig. 6), it is possible that acetylated polyamines may be back-converted to Put and Spd and then forward-converted to Spd and Spm due to excess dcSAM. These would then become available for re-acetylation by overexpressed SSAT. If sufficiently rapid, this cycling could account for the depleted acetyl-CoA pools during DFMO treatment.

As noted above, SAM pools were significantly reduced 12 h following Tet removal (Fig. 6). Repletion experiments were not feasible because, like acetyl-CoA, SAM does not penetrate cells effectively. Although SAM pools fell ~50% at 96 h (Figs. 6 and 10*B*), Spd and Spm pools did not similarly decline indicating that there was at least sufficient levels to sustain polyamine biosynthesis. A further disconnect between SAM levels and growth inhibition was noted in the finding that SAM pools remained reduced during treatment with DFMO (Fig. 10*B*), even though growth inhibition was prevented. Finally, we note that, as SAM pools declined, dcSAM pools increased in a correlative manner. Because the accumulation of dcSAM may cause growth inhibition (46), we considered that the significant rise in dcSAM seen following SSAT induction might be toxic (Fig. 6). This possibility, however, was also excluded by the finding that DFMO markedly increased dcSAM pools while preventing growth inhibition (Fig. 10*C*). Accumulation of the dcSAM metabolite, MTA, is also capable of exerting an antiproliferative effect (47, 48), but this seems unlikely in the present system, because there was no indication of Spd and Spm pool depletion, which is usually regarded as a major indication of MTA toxicity via feedback inhibition of the Spd and Spm synthases (49).

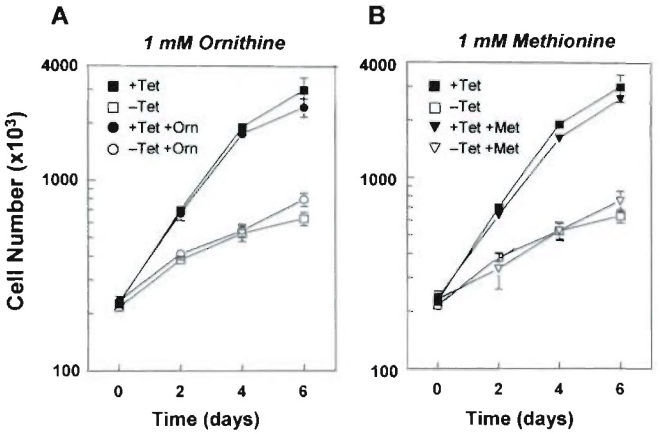

FIG. 8. **Effects of polyamine precursors on SSAT-induced cell growth inhibition.** SSAT/LNGK9-clone 53 cells grown in the presence and absence of Tet were simultaneous treated with 1 mM of the polyamine precursors, ornithine (*A*) or methionine (*B*), for the indicated time and analyzed for prevention of growth inhibition. Note that both amino acids failed to prevent SSAT-induced growth inhibition when included during Tet removal. Data represent means ± S.E., where *n* is 3.

DISCUSSION

We have previously shown that activation of polyamine catabolism by conditional overexpression of SSAT led to growth inhibition in MCF-7 breast cancer cells (31). We undertook the present study to examine whether LNCaP prostate tumor cells might respond differently to such perturbations in polyamine homeostasis. The data presented here are consistent with this possibility. Although both cell lines expressed a similar ~20-fold increase in SSAT activity, growth inhibition in MCF-7 breast carcinoma cells correlated closely with a depletion in intracellular polyamine pools (31). By contrast, growth inhibi-

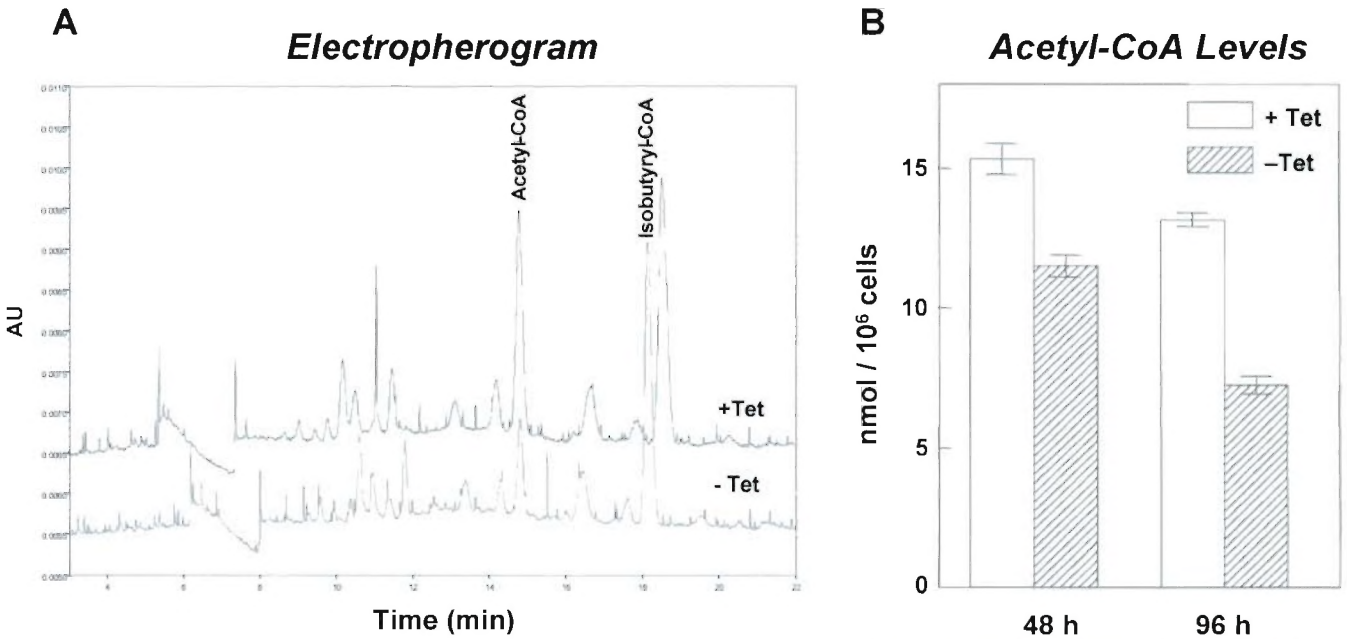

FIG. 9. **Effects of SSAT overexpression on acetyl-CoA levels.** SSAT/LNGK9-clone 53 cells were grown in the presence (*+Tet, open bar*) and absence of Tet (*−Tet, hatched bar*) for 48 and 96 h and analyzed by HPCE for acetyl-CoA. *A*, an electropherogram from HPCE showing levels of acetyl-CoA in clone 53 cells and an exogenous internal standard, isobutyryl-CoA in the presence (*+Tet*) and absence (*−Tet*) of Tet at 96 h. The internal standard isobutyryl-CoA was added to each sample to allow for calculation of loss during extraction. Note that the acetyl-CoA peak is much lower in −Tet cells compared with +Tet cells. Quantitation of the peaks (*B*) reveals a 25% decline in acetyl-CoA by 48 h and a 45% decline by 96 h in −Tet cells (*hatched bars*) when compared with their levels in +Tet cells (*open bars*). Data represent means ± S.E., where *n* is 3.

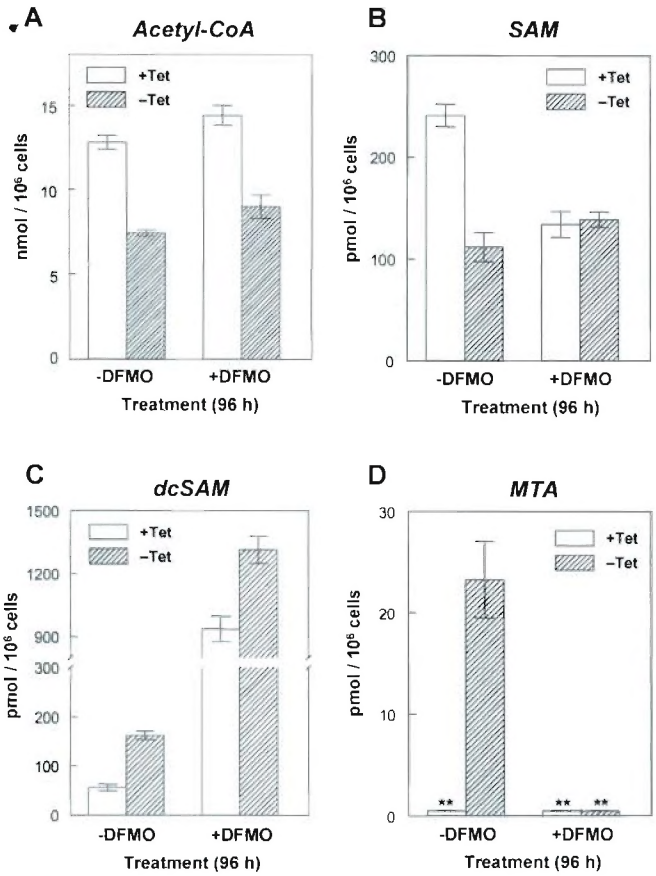

FIG. 10. **Effects of DFMO treatment on the levels of acetyl-CoA (*A*), SAM (*B*), dcSAM (*C*), and MTA (*D*) during SSAT overexpression.** SSAT/LNGK9-clone 53 cells were grown in the presence (*+Tet, open bar*) and absence of Tet (*−Tet, hatched bar*) with or without 1 mM DFMO for 96 h and analyzed by HPCE for acetyl-CoA and by HPLC for SAM, dcSAM, and MTA. Data represent means ± S.E., where n is 3.

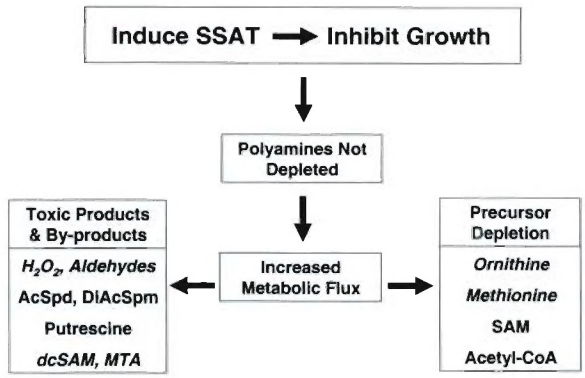

FIG. 11. **Diagrammatic representation of the possible causes of growth inhibition in SSAT overexpressing LNCaP cells.** Activation of polyamine catabolism by overexpressing SSAT causes growth inhibition in LNCaP cells, which is not accompanied by polyamine pool depletion. It is, however, associated with compensatory increase in polyamine biosynthetic activity that leads to heightened flux thru polyamine metabolism. When biosynthesis is interrupted by the ODC inhibitor, DFMO, growth inhibition is prevented (not shown), thus linking flux to the antiproliferative effect. The possible causes of growth inhibition emanating from heightened flux are presented as accumulation of product or by-product excess (*left panel*) or as depletion of critical precursors and cofactors (*right panel*). Of the product/by-product possibilities, overproduction of hydrogen peroxide (H_2O_2) and reactive aldehydes (such as acetamidopropanal), dcSAM, and MTA have been experimentally eliminated (*italic type*). Of the possible precursor possibilities, depletion of ornithine and methionine has been experimentally excluded (*italic type*). Thus, the possibilities that were not excluded and that may contribute to growth inhibition include accumulation of acetylated polyamine products, decreased levels of the polyamine aminopropyl donor, SAM, and/or a reduction in stores of the SSAT co-factor, acetyl-CoA.

tion in LNCaP prostate carcinoma cells took place in the absence of polyamine pool depletion. As will be discussed below, the difference appears to be due to the ability of LNCaP cells to metabolically compensate for activated catabolism or conversely, to the inability of MCF-7 cells to mount such a response.

The idea of activating polyamine catabolism derived from observations made with polyamine analogues (23–27). We note that conditional overexpression of SSAT produces a 10- to 20-fold increase in SSAT activity, whereas induction by polyamine analogues such as DENSPM reaches ~1000-fold in certain cell lines. A significant portion of DENSPM-induced enzyme protein, however, is inhibited by analogue binding and is unable to acetylate polyamines (50). Accumulation of acetylated products represents a better indication of SSAT functional overexpression in cells. Thus, the seemingly modest 20-fold increase in SSAT activity seen here in LNCaP cells resulted in exceedingly high levels of intracellular and extracellular acetylated polyamines, which undoubtedly had a profound impact on the metabolic equilibrium of polyamines. We also note that enzyme induction is also associated with polyamine species such as DiAcSpm that are rarely seen in cells unless SSAT is overexpressed (31) or analogue-induced (29).

It was expected that the massive acetylation of Spd and Spm and their export into the media would deplete intracellular pools as was previously seen in MCF-7 cells (31). In LNCaP cells, however, depletion of Spd and Spm was averted by a compensatory increase in polyamine biosynthesis: ODC activity rose by ~16-fold at 48 h following Tet removal and SAMDC, by ~8-fold. Thus, instead of decreasing, intracellular polyamine pools actually increased rapidly despite the diversion of huge amounts of Spd and Spm to intracellular and extracellular acetylated polyamines. Although a similar up-regulation of polyamine biosynthesis has been reported in SSAT stably transfected cell lines and most tissues of transgenic mice (51–53), it is likely to have evolve over time via a process of selection. By contrast, the increase in ODC and SAMDC activities in LNCaP cells began almost simultaneously with SSAT activation. The net effect of this response was heightened flux through the biosynthetic pathway as indicated by the decline in SAM pools and by the related rise in MTA, a by-product of the Spd and Spm synthase reactions. The relationship between this flux and cell growth was clearly established by the observation that DFMO, an inhibitor of ODC, effectively prevented SSAT-induced growth inhibition. The finding is particularly significant, because DFMO typically inhibits, rather than prevents, cell growth (16). Whether this linkage is common to prostate-derived tumor cells or whether it is MCF-7 cells that are unusual remains to be determined. If the former is confirmed, the finding is consistent with other known biochemical idiosyncrasies regarding polyamine metabolism in prostate carcinoma cell lines (11, 15).

SSAT-induced growth inhibition in the absence of polyamine pool depletion raises obvious questions regarding the basis for the antiproliferative effect. As diagrammed in Fig. 11, the high rate of metabolic flux through both the biosynthetic and catabolic arms of the pathway suggests that accumulation of pathway products or by-products may reach toxic levels (*left panel*) or that certain metabolites may become growth-limiting (*right panel*). The various possibilities that were experimentally eliminated as causes of flux-induced growth inhibition include: elaboration of PAO toxic by-products, accumulation of dcSAM, and depletion of the amino acids ornithine and methionine (Fig. 11, *italic type*). Possibilities that were not clearly elimi-

nated include high levels of acetylated polyamines and Put, depletion of SAM pools, and decreases in acetyl-CoA pools (Fig. 11).

Our HPCE analysis of acetyl-CoA pools revealed that these pools decreased by 45% during SSAT induction in LNCaP cells. To our knowledge, this is the first time that such a linkage has been demonstrated between polyamine metabolism and depletion of acetyl-CoA stores. We examined this possibility with the view that the massive amounts of acetylated polyamines being generated may render the SSAT cofactor acetyl-CoA limiting for critical cellular functions such as fatty acid synthesis, cholesterol synthesis, and histone regulation. Indeed, fatty acid synthase expression and lipidogenesis are known to be increased by androgens and highly relevant to the normal prostate biology and prostate cancer (54–56). In addition, Ettinger *et al.* (57) recently showed that androgen independence in LNCaP xenograft models is closely associated with dysregulation of enzymes that coordinately control lipogenesis and cholesterol synthesis. These various findings imply a high dependence of prostate cancer on acetyl-CoA stores.

Taken together, findings indicate that activation of polyamine catabolism at the level of SSAT leads to: (*a*) altered polyamine pool homeostasis, (*b*) a compensatory increase in polyamine biosynthesis, (*c*) heightened metabolic flux through both the biosynthetic and catabolic pathways, (*d*) synthesis of enormous quantities of acetylated polyamines, (*e*) significant depletion of critical metabolite pools such as the polyamine precursor *S*-adenosylmethionine (SAM) and the SSAT cofactor, acetyl-CoA, and (*f*) inhibition of cell growth. We emphasize that this analysis applies strictly to selective SSAT overexpression and not to enzyme induction by polyamine analogues such as DENSPM, which in addition to potently inducing SSAT also down-regulate polyamine biosynthesis and, thereby, preclude the heightened metabolic flux seen in LNCaP cells. Importantly, studies from our laboratory (58) have shown that cross-breeding SSAT transgenic mice that are genetically predisposed to develop prostate cancer (*i.e.* TRAMP mice (59) results in metabolic responses similar to those seen in LNCaP cells and leads to a marked suppression of prostate tumor outgrowth.

Although the present findings are based on an artificial system (*i.e.* conditional overexpression of SSAT), there are many pharmacological examples of SSAT induction by classes of drugs other than polyamine analogues to levels comparable to those obtained here (43). For example, we and others have shown that anticancer drugs unrelated to polyamines can also elicit very significant increases in SSAT gene expression. Maxwell *et al.* (60) found that SSAT was the most potently induced gene by the antimetabolite 5-fluorouracil from among >3000 represented in a gene profiling study of MCF-7 cells. Similarly, we have shown that SSAT mRNA is among the top 10 genes induced by the DNA-alkylating platinum compounds, oxaliplatin and cisplatin (61). Finally, studies from our laboratory (58) have shown that cross-breeding SSAT transgenic mice that are genetically predisposed to develop prostate cancer (*i.e.* TRAMP mice (59)) markedly suppressed genitourinary tumors. These findings support the possibility that selective small molecule inducers of SSAT may have therapeutic and/or preventive potential against prostate cancer.

Acknowledgments—We gratefully acknowledge the helpful discussions with Drs. Janice Sufrin and Ying Chen, and Jason A. Jell for technical assistance. We also acknowledge Mehboob Shivji for assistance in isolating acetyl-CoA.

REFERENCES

1. Porter, C. W., Regenass, U., and Bergeron, R. J. (1992) in *Falk Symposium on Polyamines in the Gastrointestinal Tract* (Dowling, R. H., Folsch, U. R., and Loser, C., eds) pp. 301–322, Kluwer Academic Publishers Group, Dordrecht, Netherlands
2. Porter, C. W., Herrera-Ornelas, L., Pera, P., Petrelli, N. F., and Mittelman, A. (1987) *Cancer* **60,** 1275–1281
3. Kramer, D. L. (1996) in *Critical Roles of Polyamines in Cancer: Basic Mechanisms and Clinical Approaches* (Nishioka, K., ed) pp. 151–189, R. G. Landes Co., New York
4. Thomas, T., and Thomas, T. J. (2003) *J. Cell Mol. Med.* **7,** 113–126
5. Thomas, T., and Thomas, T. J. (2001) *Cell Mol. Life Sci.* **58,** 244–258
6. Seiler, N. (2003) *Curr. Drug Targets* **4,** 537–564
7. Harrison, G. A. (1931) *Biochem. J.* **25,** 1885–1892
8. Mann, T. (1964) *The Biochemistry of Semen and of the Male Reproductive Tract*, John Wiley, New York, pp. 193–200
9. Pegg, A. E., and Williams-Ashman, H. G. (1968) *Biochem. J.* **108,** 533–539
10. Williams-Ashman, H. G., and Canellakis, Z. N. (1979) *Perspect. Biol. Med.* **22,** 421–453
11. Mi, Z., Kramer, D. L., Miller, J. T., Bergeron, R. J., Bernacki, R., and Porter, C. W. (1998) *Prostate* **34,** 51–60
12. Rhodes, D. R., Barrette, T. R., Rubin, M. A., Ghosh, D., and Chinnaiyan, A. M. (2002) *Cancer Res.* **62,** 4427–4433
13. Bettuzzi, S., Davalli, P., Astancolle, S., Carani, C., Madeo, B., Tampieri, A., Corti, A., Saverio, B., Pierpaola, D., Serenella, A., Cesare, C., Bruno, M., Auro, T., and Arnaldo, C. (2000) *Cancer Res.* **60,** 28–34
14. Heston, W. D., Watanabe, K. A., Pankiewicz, K. W., and Covey, D. F. (1987) *Biochem. Pharmacol.* **36,** 1849–1852
15. Heston, W. D. (1991) *Cancer Surv.* **11,** 217–238
16. Mamont, P. S., Duchesne, M. C., Grove, J., and Bey, P. (1978) *Biochem. Biophys. Res. Commun.* **81,** 58–66
17. Regenass, U., Mett, H., Stanek, J., Mueller, M., Kramer, D., and Porter, C. W. (1994) *Cancer Res.* **54,** 3210–3217
18. Kramer, D. L., Khomutov, R. M., Bukin, Y. V., Khomutov, A. R., and Porter, C. W. (1989) *Biochem. J.* **259,** 325–331
19. Danzin, C., Marchal, P., and Casara, P. (1990) *Biochem. Pharmacol.* **40,** 1499–1503
20. Gupta, S., Ahmad, N., Marengo, S. R., MacLennan, G. T., Greenberg, N. M., and Mukhtar, H. (2000) *Cancer Res.* **60,** 5125–5133
21. Bergeron, R. J., Feng, Y., Weimar, W. R., McManis, J. S., Dimova, H., Porter, C., Raisler, B., and Phanstiel, O. (1997) *J. Med. Chem.* **40,** 1475–1494
22. Casero, R. A., Jr., Celano, P., Ervin, S. J., Porter, C. W., Bergeron, R. J., and Libby, P. R. (1989) *Cancer Res.* **49,** 3829–3833
23. Libby, P. R., Bergeron, R. J., and Porter, C. W. (1989) *Biochem. Pharmacol.* **38,** 1435–1442
24. Casero, R. A., Jr., Ervin, S. J., Celano, P., Baylin, S. B., and Bergeron, R. J. (1989) *Cancer Res.* **49,** 639–643
25. Shappell, N. W., Miller, J. T., Bergeron, R. J., and Porter, C. W. (1992) *Anticancer Res.* **12,** 1083–1089
26. Pegg, A. E., Wechter, R., Pakala, R., and Bergeron, R. J. (1989) *J. Biol. Chem.* **264,** 11744–11749
27. Porter, C. W., Ganis, B., Libby, P. R., and Bergeron, R. J. (1991) *Cancer Res.* **51,** 3715–3720
28. McCloskey, D. E., and Pegg, A. E. (2000) *J. Biol. Chem.* **275,** 28708–28714
29. Chen, Y., Kramer, D. L., Li, F., and Porter, C. W. (2003) *Oncogene* **22,** 4964–4972
30. Chen, Y., Kramer, D. L., Jell, J., Vujcic, S., and Porter, C. W. (2003) *Mol. Pharmacol.* **64,** 1153–1159
31. Vujcic, S., Halmekyto, M., Diegelman, P., Gan, G., Kramer, D. L., Janne, J., and Porter, C. W. (2000) *J. Biol. Chem.* **275,** 38319–38328
32. Liu, G., Chen, J., Che, P., and Ma, Y. (2003) *Anal. Chem.* **75,** 78–82
33. Gossen, M., and Bujard, H. (1992) *Proc. Natl. Acad. Sci. U. S. A.* **89,** 5547–5551
34. Gschwend, J. E., Fair, W. R., and Powell, C. T. (1997) *Prostate* **33,** 166–176
35. Fogel-Petrovic, M., Shappell, N. W., Bergeron, R. J., and Porter, C. W. (1993) *J. Biol. Chem.* **268,** 19118–19125
36. Xiao, L., Celano, P., Mank, A. R., Pegg, A. E., and Casero, R. A., Jr. (1991) *Biochem. Biophys. Res. Commun.* **179,** 407–415
37. Porter, C. W., Cavanaugh, P. F., Jr., Stolowich, N., Ganis, B., Kelly, E., and Bergeron, R. J. (1985) *Cancer Res.* **45,** 2050–2057
38. Kramer, D., Mett, H., Evans, A., Regenass, U., Diegelman, P., and Porter, C. W. (1995) *J. Biol. Chem.* **270,** 2124–2132
39. Kramer, D., Stanek, J., Diegelman, P., Regenass, U., Schneider, P., and Porter, C. W. (1995) *Biochem. Pharmacol.* **50,** 1433–1443
40. Yarlett, N., and Bacchi, C. J. (1988) *Mol. Biochem. Parasitol.* **27,** 1–10
41. Seiler, N., Bolkenius, F. N., and Knodgen, B. (1980) *Biochim. Biophys. Acta* **633,** 181–190
42. Seiler, N., Bolkenius, F. N., and Rennert, O. M. (1981) *Med. Biol.* **59,** 334–346
43. Seiler, N. (1987) *Can. J. Physiol. Pharmacol.* **65,** 2024–2035
44. Ha, H. C., Woster, P. M., Yager, J. D., and Casero, R. A., Jr. (1997) *Proc. Natl. Acad. Sci. U. S. A.* **94,** 11557–11562
45. Devens, B. H., Weeks, R. S., Burns, M. R., Carlson, C. L., and Brawer, M. K. (2000) *Prostate Cancer Prostatic Dis.* **3,** 275–279
46. Pegg, A. E. (1984) *Biochem. J.* **224,** 29–38
47. Yamanaka, H., Kubota, M., and Carson, D. A. (1987) *Cancer Res.* **47,** 1771–1774
48. Williams-Ashman, H. G., Seidenfeld, J., and Galletti, P. (1982) *Biochem. Pharmacol.* **31,** 277–288
49. Pajula, R. L., and Raina, A. (1979) *FEBS Lett.* **99,** 343–345
50. Libby, P. R., Ganis, B., Bergeron, R. J., and Porter, C. W. (1991) *Arch. Biochem. Biophys.* **284,** 238–244
51. Pietila, M., Alhonen, L., Halmekyto, M., Kanter, P., Janne, J., and Porter, C. W. (1997) *J. Biol. Chem.* **272,** 18746–18751
52. Alhonen, L., Karppinen, A., Uusi-Oukari, M., Vujcic, S., Korhonen, V. P., Halmekyto, M., Kramer, D. L., Hines, R., Janne, J., and Porter, C. W. (1998) *J. Biol. Chem.* **273,** 1964–1969
53. McCloskey, D. E., Coleman, C. S., and Pegg, A. E. (1999) *J. Biol. Chem.* **274,**

6175–6182
54. Swinnen, J. V., Esquenet, M., Goossens, K., Heyns, W., and Verhoeven, G. (1997) *Cancer Res.* **57,** 1086–1090
55. Swinnen, J. V., Ulrix, W., Heyns, W., and Verhoeven, G. (1997) *Proc. Natl. Acad. Sci. U. S. A.* **94,** 12975–12980
56. Swinnen, J. V., Vanderhoydonc, F., Elgamal, A. A., Eelen, M., Vercaeren, I., Joniau, S., Van Poppel, H., Baert, L., Goossens, K., Heyns, W., and Verhoeven, G. (2000) *Int. J. Cancer* **88,** 176–179
57. Ettinger, S. L., Sobel, R., Whitmore, T. G., Akbari, M., Bradley, D. R., Gleave, M. E., and Nelson, C. C. (2004) *Cancer Res.* **64,** 2212–2221
58. Kee, K., Vujcic, S., Kisiel, N., Diegelman, P., Kramer, D. L., and Porter, C. W. (2003) *Proc. Am. Assoc. Cancer Res.* **44,** 1277
59. Greenberg, N. M., DeMayo, F., Finegold, M. J., Medina, D., Tilley, W. D., Aspinall, J. O., Cunha, G. R., Donjacour, A. A., Matusik, R. J., and Rosen, J. M. (1995) *Proc. Natl. Acad. Sci. U. S. A.* **92,** 3439–3443
60. Maxwell, P. J., Longley, D. B., Latif, T., Boyer, J., Allen, W., Lynch, M., McDermott, U., Harkin, D. P., Allegra, C. J., and Johnston, P. G. (2003) *Cancer Res.* **63,** 4602–4606
61. Hector, S., Porter, C. W., Kramer, D. L., Clark, K., Chen, Y., and Pendyala, L. (2004) *Mol. Cancer Ther.*, in press